https://doi.org/10.5194/egusphere-2026-3629
Preprint. Discussion started: 26 June 2026

Eulerian and Lagrangian Assessment of Arctic Surface Current Products Using Drifter Observations

Aleida Rosquete-Estevez[1,★], Júlia Crespin[1,★], Luis Yubero[2,3], Ana María Mancho[2], and Marta Umbert[1]

[1]Barcelona Polar Lab, Department of Physical and Technological Oceanography, Institute of Marine Sciences (ICM), CSIC, Barcelona, Spain
[2]Instituto de Ciencias Matemáticas (ICMAT), CSIC, Madrid, Spain
[3]Escuela Técnica Superior de Ingenieros de Telecomunicación, Universidad Politécnica de Madrid, Madrid, Spain
★These authors contributed equally to this work.

Correspondence: Marta Umbert (mumbert@icm.csic.es)

Abstract. Accurate Arctic surface current estimates are needed to quantify freshwater redistribution, upper-ocean connectivity, and Arctic–North Atlantic exchanges, but validating them is difficult given sparse observations, sea-ice cover, and overlapping dynamical processes. This study evaluates six widely used products against drogued drifters from the Global Drifter Program (2011–2021): AVISO altimetry-derived geostrophic currents, NeurOST machine-learning reconstructions, GlobCurrent and OSCAR multi-observational/mixed-layer total currents, and the GLORYS and TOPAZ reanalyses. Skill is assessed with complementary Eulerian point-wise metrics and Lagrangian trajectory diagnostics, including a Lagrangian Uncertainty Quantification (LUQ) framework. Eulerian results show marked regional and seasonal contrasts. NeurOST and OSCAR agree best with drifter velocities, GlobCurrent and GLORYS show intermediate skill, TOPAZ has weaker near-surface speed agreement, and AVISO underestimates current intensity and variability. Products incorporating additional observational constraints, wind-driven contributions, or mixed-layer dynamics outperform altimetry-only geostrophic estimates, especially in regions shaped by mesoscale variability, bathymetry, sea ice, and narrow gateways. The Lagrangian analysis shows that good local velocity agreement does not guarantee realistic transport: small velocity differences accumulate along trajectories, producing large deviations in pathways, retention, and connectivity. LUQ diagnostics indicate part of this mismatch reflects intrinsic transport variability and initial-condition sensitivity rather than product error alone. The authors conclude that Eulerian validation must be complemented by Lagrangian, uncertainty-aware diagnostics for studies of freshwater pathways, tracer transport, and Arctic connectivity.

1 Introduction

The Arctic Ocean is undergoing rapid transformations driven by climate warming, including sea-ice retreat, enhanced freshwater input from rivers, Greenland runoff and sea-ice melt, and changes in ocean circulation (Serreze and Francis, 2006; Haine et al., 2015). These processes modify upper-ocean stratification, freshwater storage, and exchanges with the North Atlantic, with potential implications for regional climate and the Atlantic Meridional Overturning Circulation (Rahmstorf et al., 2015). Because the redistribution and export of freshwater—particularly within major features such as the Beaufort Gyre and through

https://doi.org/10.5194/egusphere-2026-3629
Preprint. Discussion started: 26 June 2026

Arctic gateways—are strongly controlled by upper-ocean currents (Proshutinsky et al., 2009, 2019), accurate estimates of near-surface circulation are essential for quantifying Arctic transport pathways and understanding the evolving Arctic climate system.

Satellite observations provide a unique capability to monitor ocean circulation over broad spatial and temporal scales. Near-surface currents can be derived from sea surface height (SSH) gradients using satellite altimetry (Fu, 2010), while other approaches combine multiple sources of information, including wind stress, sea surface temperature, drifter trajectories, and ocean model constraints (Lagerloef et al., 1999; Bonjean and Lagerloef, 2002; Dohan, 2017). However, estimating surface currents in the Arctic remains particularly challenging because of seasonal sea-ice cover, reduced satellite sampling at high latitudes, limited in situ observations, and the coexistence of geostrophic, wind-driven, mixed-layer, and ice-ocean processes acting across a wide range of scales (Armitage et al., 2016; Villas Bôas et al., 2019).

Several surface current products are currently available, but they differ substantially in their dynamical assumptions, observational constraints, and effective depth representation. Altimetry-based products such as AVISO provide surface geostrophic currents derived from SSH gradients (Traon and Dibarboure, 2002). Machine-learning approaches such as NeurOST reconstruct sea surface height and geostrophic currents by combining sparse nadir altimetry observations with high-resolution sea surface temperature information (Martin et al., 2024). Other products, such as OSCAR and GlobCurrent, provide total or near-surface currents by combining geostrophic estimates with wind-driven or mixed-layer contributions (Bonjean and Lagerloef, 2002; Dohan, 2017; Rio et al., 2014). Ocean reanalyses, including GLORYS and TOPAZ, provide dynamically consistent current fields based on ocean model physics and data assimilation (Lellouche et al., 2021; Sakov et al., 2012). These products are widely used to study ocean circulation, tracer transport, and freshwater pathways, yet their performance in the Arctic remains insufficiently constrained because of the scarcity and uneven distribution of independent observations (Armitage et al., 2017).

Drifting buoys provide a valuable reference for near-surface currents because they directly sample the Lagrangian motion of water parcels (Lumpkin and Pazos, 2007). In particular, drogued drifters are designed to follow the motion of the upper ocean, providing an observational benchmark for evaluating current products. However, drifter observations are sparse in the Arctic and are mainly concentrated in seasonally ice-free regions, which limits validation in the central Arctic and other persistently ice-covered areas. In addition, drifters sample the flow at an effective depth that may differ from the depth or dynamical component represented by individual current products, introducing an additional source of uncertainty in intercomparison studies (Lumpkin et al., 2013).

Traditional validation studies rely on Eulerian metrics based on point-wise comparisons between observed and modeled velocities, using statistical indicators such as root-mean-square error, bias, and correlation (Chiswell and Rickard, 2008; Rio et al., 2014; Sudre et al., 2023). These metrics provide useful information on local velocity agreement, but they do not necessarily evaluate whether a velocity field reproduces realistic transport pathways. This distinction is particularly important in the Arctic, where small velocity differences can accumulate over time and lead to large deviations in particle trajectories, freshwater redistribution, and export pathways.

Assessing transport skill therefore requires a complementary perspective that focuses directly on the evolution of fluid parcels rather than on local velocity agreement alone. Lagrangian approaches based on trajectory analysis offer a valuable complement

https://doi.org/10.5194/egusphere-2026-3629
Preprint. Discussion started: 26 June 2026

to Eulerian methods because they evaluate the ability of current products to reproduce observed transport pathways (Vastano and Barron, 1994; Barron et al., 2007; Liu and Weisberg, 2011; Van Sebille et al., 2018). Additionally, an interesting approach to studying transport pathways is to identify geometrical structures on the ocean surface that organize fluid trajectories into regions exhibiting qualitatively different dynamical behaviour. These geometrical structures are dynamically invariant and are known as Lagrangian Coherent Structures (LCSs), serving as the signature of the transport produced by ocean currents. This framework has been used to assess whether transport inferred from different datasets is consistent with drifter observations (Shadden et al., 2009; Mendoza et al., 2014) or to compare transport predictions from alternative ocean products in search-and-rescue operations (García-Garrido et al., 2015). However, the use of LCSs for the assessment of ocean datasets has remained largely qualitative. More recently, advances in Lagrangian diagnostics have led to quantitative approaches that link deviations between transport predictions and observations to the underlying LCSs. This has resulted in the development of the Lagrangian Uncertainty Quantification (LUQ) framework (García-Sánchez et al., 2021, 2022b, 2023, 2025). LUQ enables trajectory-based comparisons that quantify deviations from ground truth while accounting for the fact that these deviations are not randomly distributed, but structured by the underlying flow dynamics. This perspective is particularly relevant in dynamically complex regions, where nearby trajectories may naturally diverge because of mesoscale variability, transport barriers, or recirculating flow structures. An uncertainty-aware Lagrangian framework therefore, provides a physically meaningful complement to classical Eulerian validation in the Arctic Ocean.

In this study, we evaluate six Arctic surface current products using both Eulerian and Lagrangian diagnostics over the 2011–2021 period. Drifter observations from the Global Drifter Program (GDP) are used as an independent reference dataset to assess altimetry-derived geostrophic currents, machine-learning geostrophic reconstructions, total surface current products, and ocean reanalyses. In addition to classical validation metrics, we apply a LUQ framework to quantify uncertainty in trajectory-based comparisons and to evaluate the consistency of simulated transport pathways across contrasting Arctic circulation regimes. Through this comprehensive intercomparison, this work contributes to the systematic evaluation of polar ocean reanalyses, providing critical guidance on their physical consistency and performance limitations for tracer and transport applications.

The objectives of this study are to: (1) assess the capability of different Arctic surface current products to reproduce observed near-surface circulation; (2) compare the information provided by Eulerian and Lagrangian validation approaches; and (3) evaluate the added value of uncertainty-aware Lagrangian diagnostics for assessing Arctic transport pathways in data-sparse and dynamically complex regions.

2 Data

The analysis is restricted to the Arctic region, here defined as the oceanic domain north of 50°N. The study period spans 2011–2021, corresponding to the common temporal availability of the surface current products evaluated in this work and the drifter observations used for validation.

The evaluated products differ substantially in their dynamical content, observational constraints, spatial coverage, and effective sampling depth. AVISO and NeurOST provide surface geostrophic currents derived from sea surface height informa-

https://doi.org/10.5194/egusphere-2026-3629
Preprint. Discussion started: 26 June 2026

tion, although NeurOST further uses a machine-learning reconstruction constrained by nadir altimetry and high-resolution sea surface temperature. GlobCurrent and OSCAR provide total or near-surface current estimates that include wind-driven or mixed-layer contributions, whereas GLORYS and TOPAZ are ocean reanalyses based on numerical model dynamics and data assimilation. These differences are essential for interpreting the comparison with drogued drifters, which sample the motion of the upper ocean at an effective depth of approximately 15 m (Lumpkin and Pazos, 2007). Therefore, the validation should not be interpreted as a comparison of strictly equivalent physical quantities, but rather as an assessment of how well each product reproduces the near-surface motion observed by drifters.

2.1 Satellite-Derived Current Products

2.1.1 AVISO Arctic Ocean

The AVISO Arctic Ocean product provides surface geostrophic currents derived from sea surface height gradients. We used the SSALTO/DUACS Experimental Level-4 Arctic Ocean product distributed by AVISO+ and the Copernicus Marine Service (CMEMS) (Lellouche et al., 2021). The dataset combines observations from Sentinel-3, CryoSat-2, and SARAL/AltiKa through an optimal interpolation framework adapted to high latitudes (Prandi et al., 2021).

The product includes Sea Level Anomaly (SLA), Absolute Dynamic Topography (ADT), and the corresponding zonal and meridional geostrophic velocity components (u_g, v_g) derived from horizontal ADT gradients. Because the currents are computed assuming geostrophic balance, AVISO primarily represents the large-scale balanced component of the surface circulation and does not explicitly include wind-driven, inertial, or other ageostrophic contributions.

The velocity fields (Fig. 1a) are provided every 3 days on a 25-km EASE2 grid, extending from 50°N to approximately 88°N. This Arctic configuration incorporates processing specifically designed for high-latitude altimetry, including the use of sea-level returns within sea-ice leads, which improves spatial coverage in seasonally ice-covered regions. Nevertheless, uncertainties remain larger in areas affected by persistent sea-ice cover, weak dynamic topography gradients, and sparse satellite sampling.

Further details are available through the CMEMS platform at: https://doi.org/10.24400/527896/a01-2020.001 (Lellouche et al., 2021).

2.1.2 GlobCurrent

GlobCurrent is a multi-observational surface current product developed within the European Space Agency (ESA) GlobCurrent project. It combines satellite-derived geostrophic currents with wind-driven Ekman currents to provide estimates of total ocean surface velocity (Fig. 1b). The product includes both reprocessed (REP) long-term archives and near-real-time (NRT) current estimates.

The total horizontal velocity fields are obtained by adding geostrophic currents derived from satellite altimetry to Ekman currents estimated from wind stress. The dataset provides zonal and meridional velocity components at both the surface (0 m) and 15 m depth, together with the corresponding geostrophic and Ekman components and associated uncertainty estimates. In

https://doi.org/10.5194/egusphere-2026-3629
Preprint. Discussion started: 26 June 2026

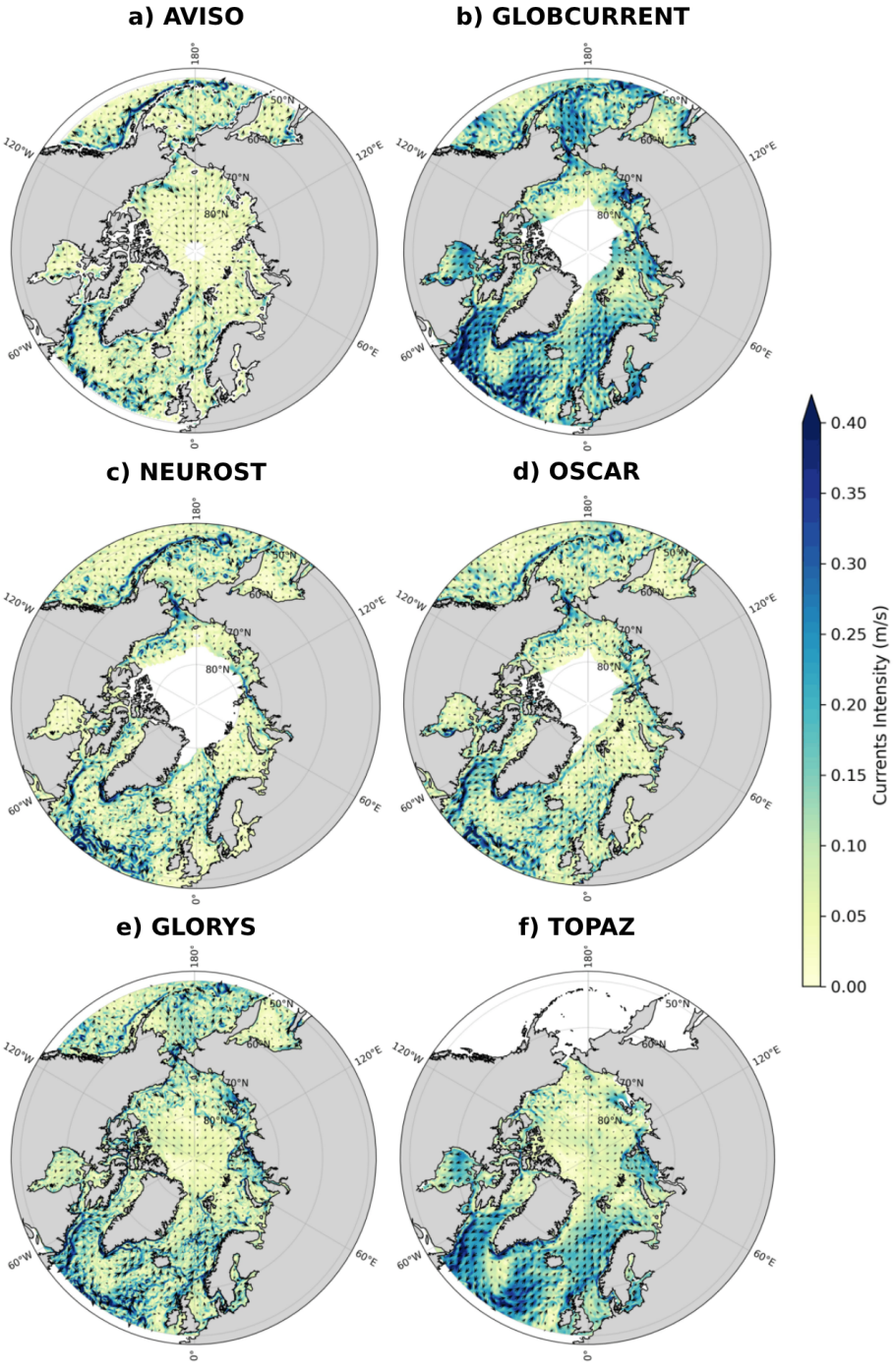

Figure 1. Surface geostrophic currents on 4 October 2016 from six products: a) AVISO, b) GLOBCURRENT, c) NEUROST, d) OSCAR, e) GLORYS, and f) TOPAZ. Vectors show current direction and speed, color shading indicates speed (m s^{-1}). All fields are plotted on the same grid and color scale to facilitate comparison; land and masked regions are shown in gray.

https://doi.org/10.5194/egusphere-2026-3629
Preprint. Discussion started: 26 June 2026

this study, we use the total current fields at 15 m depth, which are the most directly comparable to the nominal drogue depth of the GDP drifters.

GlobCurrent is distributed on a regular $1/4^\circ$ grid at hourly temporal resolution, with daily and monthly averaged fields also available. Because it explicitly incorporates both geostrophic and wind-driven contributions, GlobCurrent is expected to better represent the near-surface motion sampled by drifters than purely geostrophic products. However, the combination of multiple observational and modeled components may also introduce spatial smoothing and uncertainties, particularly in regions affected by strong mesoscale variability, sea-ice influence, or narrow topographic currents.

Further configuration details are accessible through the CMEMS platform at: https://doi.org/10.48670/mds-00327 (Rio et al., 2014).

2.1.3 OSCAR

The Ocean Surface Current Analyses Real-time (OSCAR) product provides global near-surface ocean current estimates derived from satellite observations of sea surface topography, ocean vector winds, and sea surface temperature (Bonjean and Lagerloef, 2002; Lagerloef et al., 1999). In this study, we use Version 2 of the dataset distributed by the NASA Physical Oceanography Distributed Active Archive Center (PO.DAAC) (Dohan, 2021).

Unlike purely geostrophic products, OSCAR combines satellite observations with a simplified dynamical model of the turbulent upper-ocean mixed layer (Dohan, 2017). The resulting currents include geostrophic, wind-driven, and thermal-wind contributions and are representative of the upper 30 m of the water column. This makes OSCAR particularly relevant for comparison with drogued drifters, which sample the upper-ocean flow rather than the purely geostrophic surface component.

The dataset provides daily current fields on a regular $0.25^\circ \times 0.25^\circ$ grid covering the global ocean from 1993 onward. The gridded fields include total zonal and meridional velocity components (u, v), together with the corresponding geostrophic contributions (u_g, v_g). Because OSCAR relies on satellite vector winds and radiometer fields, it masks ice-covered regions, limiting its Arctic coverage to ice-free basins and seasonal marginal ice zones.

The inclusion of wind-driven and mixed-layer dynamics is expected to improve the representation of the near-surface motion sampled by drifters. However, the simplified mixed-layer formulation, spatial smoothing, and sea-ice masking may limit its ability to reproduce sharp fronts, narrow boundary currents, and mesoscale variability in dynamically active Arctic regions.

Further details are available at: https://doi.org/10.5067/OSCAR-25F20 (Dohan, 2021).

2.1.4 NeurOST

NeurOST is a data-driven, machine-learning-based reconstruction of sea surface height and surface geostrophic currents developed by the University of Washington and the Jet Propulsion Laboratory (JPL). The product (Fig. 1c) is generated using a neural network trained with sparse Level-3 nadir altimetry observations and high-resolution sea surface temperature (SST) fields from the Multi-scale Ultra-high Resolution (MUR) SST product (Martin et al., 2024).

By exploiting the complementary information contained in altimetric sea level observations and SST patterns, NeurOST aims to reconstruct finer-scale SSH and geostrophic current structures than those typically resolved by conventional optimal

https://doi.org/10.5194/egusphere-2026-3629
Preprint. Discussion started: 26 June 2026

interpolation methods. The product provides daily maps of sea surface height and the corresponding surface geostrophic velocity components at global scale (OSTST, 2024).

This approach is particularly relevant for the Arctic Ocean, where satellite altimetry coverage is sparse, sea-ice conditions complicate SSH retrievals, and mesoscale circulation structures are often poorly represented in standard gridded products. However, because NeurOST provides geostrophic currents, it does not explicitly resolve wind-driven, inertial, or other ageostrophic components of the near-surface flow sampled by drifters. Its performance therefore depends both on the quality of the underlying altimetry and SST constraints and on the extent to which the observed drifter motion is dominated by geostrophic dynamics.

Further information is available at: https://doi.org/10.5067/NEURO-STV24 (OSTST, 2024).

2.2 Ocean Circulation Model Reanalysis

2.2.1 GLORYS

The Global Ocean Reanalysis and Simulation product GLORYS12v1 (GLORYS) is a global eddy-resolving ocean reanalysis produced by Mercator Ocean International and distributed through CMEMS. The reanalysis is based on the Nucleus for European Modelling of the Ocean (NEMO) ocean general circulation model, configured on a $1/12^\circ$ horizontal grid with 50 vertical levels.

GLORYS combines ocean model dynamics with data assimilation of multiple observational datasets, including along-track satellite altimetry, sea surface temperature, sea-ice concentration, and in situ temperature and salinity profiles (Pujol et al., 2016; Reynolds et al., 2007; Lellouche et al., 2021). Atmospheric forcing is provided by ECMWF reanalyses, using ERA-Interim before 2019 and ERA5 thereafter.

Unlike purely satellite-derived current products, GLORYS provides a dynamically consistent three-dimensional representation of the ocean circulation, including interactions between the surface and subsurface ocean. This makes it useful for representing large-scale and topographically constrained Arctic circulation features. However, model parameterizations, finite resolution, and the assimilation procedure may smooth small-scale currents, fronts, and transport barriers that are relevant for Lagrangian transport.

In this study, we use daily surface current velocities from the *GLOBAL_MULTIYEAR_PHY_001_030* product distributed through CMEMS at: https://doi.org/10.48670/moi-00021 (Fig. 1e). Although GLORYS provides subsurface velocity fields that could more closely match the 15 m nominal depth of the drogued drifters, we specifically extract the uppermost surface layer. This choice is made to ensure methodological consistency across all datasets, enabling a direct and fair comparison with the satellite-derived surface products evaluated in this study.

2.2.2 TOPAZ

The Arctic Ocean Physics Reanalysis product TOPAZ4b (TOPAZ) (Sakov et al., 2012) is a regional coupled ocean–sea-ice reanalysis covering the Arctic and North Atlantic Oceans. It is operated by the Nansen Environmental and Remote Sensing

https://doi.org/10.5194/egusphere-2026-3629
Preprint. Discussion started: 26 June 2026

Center (NERSC) and distributed through CMEMS. The system is based on the Hybrid Coordinate Ocean Model (HYCOM) (Bleck, 2002), coupled to a sea-ice model that includes thermodynamic formulations and elastic-viscous-plastic rheology (Drange and Simonsen, 1996; Hunke and Dukowicz, 1997).

TOPAZ uses data assimilation based on the Deterministic Ensemble Kalman Filter (DEnKF) (Sakov and Oke, 2008), assimilating a range of satellite and in situ observations, including sea level anomaly, sea surface temperature, sea-ice concentration, sea-ice drift, and temperature and salinity profiles. The model is configured on a regional Arctic grid with a horizontal spacing of approximately 11–16 km and 50 hybrid vertical layers.

As a regional ocean–ice reanalysis, TOPAZ provides a dynamically consistent representation of Arctic circulation and ice-ocean interactions. This makes it particularly relevant for high-latitude applications, although its finite resolution, data assimilation strategy, and model parameterizations may affect the representation of near-surface currents, narrow gateways, and small-scale transport barriers.

In this study, we use daily surface current velocities from the *ARCTIC_MULTIYEAR_PHY_002_003* product distributed through CMEMS at: https://doi.org/10.48670/moi-00007 (Fig. 1f). As with GLORYS product, despite the availability of vertical levels near the drifter drogue depth, we restrict our analysis to the uppermost surface currents. This ensures a uniform evaluation framework, keeping the analysis physically and methodologically consistent with the satellite altimetry-derived products.

2.3 Global Drifter Program

Independent in situ drifter observations were used as the reference dataset for validation. Drifters provide Lagrangian measurements by following the motion of water parcels, and therefore offer a direct observational benchmark for assessing near-surface ocean currents and transport pathways.

The observational trajectories used in this study were obtained from the Global Drifter Program (GDP), managed by the National Oceanic and Atmospheric Administration (NOAA) Atlantic Oceanographic and Meteorological Laboratory (AOML). The GDP is part of the Global Ocean Observing System and maintains a global array of satellite-tracked drifting buoys designed to measure ocean currents and sea surface temperature (Lumpkin and Pazos, 2007). The drifters used here are drogued at approximately 15 m depth, allowing them to follow the motion of the upper ocean and providing a suitable reference for the evaluated near-surface current products.

We used the quality-controlled 6-hour interpolated drifter dataset distributed by the NOAA AOML Drifter Data Assembly Center. The dataset provides satellite-tracked trajectory data that have undergone quality control and interpolation procedures (Lumpkin and Centurioni, 2019). Each trajectory record includes the drifter identification number, time, geographical position, zonal and meridional velocity components, sea surface temperature, and metadata describing drogue presence and quality-control flags.

In the present work, the drifter velocity components were used for the Eulerian validation of the current products, while the drifter positions were used to reconstruct observed trajectories and compute the corresponding Lagrangian transport diagnostics.

https://doi.org/10.5194/egusphere-2026-3629
Preprint. Discussion started: 26 June 2026

The dataset is publicly available through the NOAA National Centers for Environmental Information (NCEI) and can be accessed at: https://doi.org/10.25921/7ntx-z961 (Lumpkin and Centurioni, 2010).

3 Methods

3.1 Processing of the drifter trajectories

The drifter data used in this study cover the period 2011–2021, consistent with the temporal availability of the evaluated current products. Only trajectories located north of 50°N were retained to match the Arctic domain considered in this work. The original dataset contained trajectories from 1679 drifters. After applying the processing and quality-control steps described below, 742 drogued drifters were retained for the analysis. Their spatial distribution is shown in Fig. 2.

The dataset was processed using a Python workflow designed to extract, separate, and clean individual drifter trajectories. Records associated with each drifter were sorted chronologically, and only drogued observations were retained to ensure that the measurements represented the motion of the upper ocean at approximately 15 m depth. Basic quality control was applied by removing missing values and unrealistic measurements based on velocity-error information and maximum-speed thresholds.

Because the GDP dataset is provided at 6-hour temporal resolution, interpolation was only applied when temporal gaps occurred within otherwise valid trajectories, in order to reconstruct regular 6-hour time series. A low-pass filter was then applied to the zonal and meridional velocity components to remove variability at time scales shorter than 36 hours, consistent with the daily temporal resolution of most products evaluated against the drifter observations. The filtered data were subsequently averaged to daily values.

The resulting drifter records include time, latitude, longitude, eastward and northward velocity components, velocity-error estimates, speed magnitude, direction, and metadata required to identify each trajectory. The daily velocity components were used for the Eulerian validation, while the corresponding positions were used to reconstruct observed trajectories for the Lagrangian analysis.

3.2 Eulerian Validation Metrics

Classical Eulerian validation metrics were computed to evaluate the agreement between the different surface current products and drifter-derived near-surface velocities. The analysis includes root-mean-square error (RMSE), mean bias, Pearson correlation coefficient, directional statistics, and current speed distributions (Chiswell and Rickard, 2008). These diagnostics quantify the capability of each product to reproduce the magnitude, variability, and direction of the observed upper-ocean circulation.

The validation was based on an in situ collocation approach. For each drifter observation, the nearest available surface current estimate from each product was extracted in space and time. This procedure enables direct point-wise comparison between observed and product-derived velocities under consistent sampling conditions.

Because the evaluated datasets represent different dynamical components and effective sampling depths, the collocation should not be interpreted as a comparison of strictly equivalent physical quantities. AVISO and NeurOST primarily represent

https://doi.org/10.5194/egusphere-2026-3629
Preprint. Discussion started: 26 June 2026

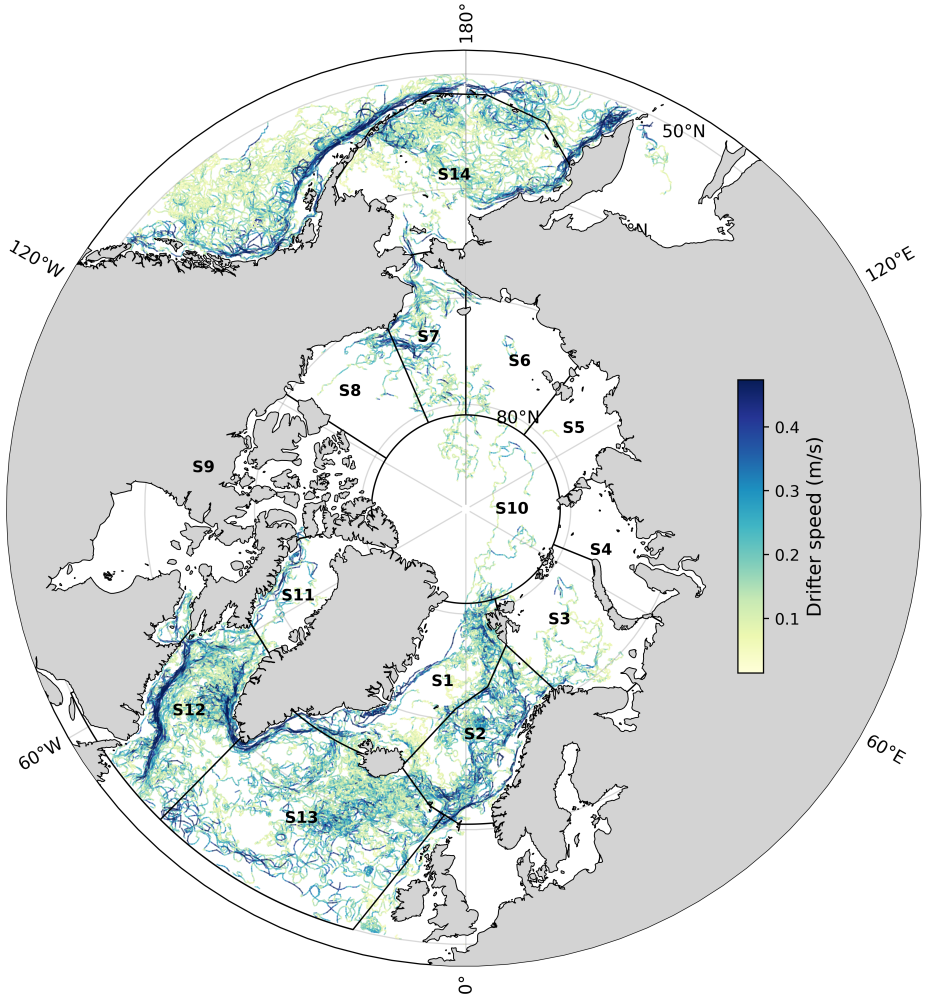

Figure 2. Trajectories of the 742 drifters retained after data cleaning. The tracks illustrate the spatial coverage of the dataset over the Arctic region during the study period and the velocity of the drifter trajectories. The geographical regions used for the regional Eulerian validation (S1–S14) are also indicated.

https://doi.org/10.5194/egusphere-2026-3629
Preprint. Discussion started: 26 June 2026

surface geostrophic circulation, GlobCurrent and OSCAR include wind-driven or mixed-layer contributions, and GLORYS and TOPAZ provide model-based reanalysis currents. In contrast, the GDP drifters sample the motion of the upper ocean at an effective depth of approximately 15 m. Nevertheless, this framework provides a practical assessment of how well each product reproduces the near-surface circulation observed by drifters.

Drifter observations are not homogeneously distributed across the Arctic Ocean. Most trajectories are concentrated in open-ocean and seasonally ice-free regions, whereas observations remain sparse in areas affected by persistent sea-ice cover (Fig. 2). Consequently, the validation statistics partly reflect the uneven spatial and seasonal sampling of the observational dataset.

The Eulerian evaluation was conducted at multiple levels. First, global statistics were computed by aggregating all collocated observations over the full Arctic domain. Second, monthly and seasonal statistics were computed to assess temporal variations in product skill. Finally, the analysis was repeated for the geographical regions defined in Fig. 2, allowing regional differences in performance to be evaluated across the Greenland Sea (S1), Norwegian Sea (S2), Barents Sea (S3), Kara Sea (S4), Laptev Sea (S5), East Siberian Sea (S6), Chukchi Sea (S7), Beaufort Sea (S8), Canadian Archipelago (S9), Central Arctic (S10), Baffin Bay (S11), Labrador Sea (S12), Subpolar North Atlantic (S13), and Bering Sea (S14).

Although Eulerian metrics provide useful information on local velocity agreement, they do not directly evaluate whether a velocity field reproduces realistic transport pathways. In the Arctic Ocean, relatively small velocity differences may accumulate over time and lead to large deviations in particle trajectories and freshwater transport pathways. For this reason, the Eulerian analysis is complemented with the Lagrangian validation framework described in the following section.

Regional statistics in poorly sampled areas should be interpreted with caution because the number of collocated observations may be limited by sea-ice conditions, reduced drifter coverage, or limited product availability.

3.3 Lagrangian Validation Framework

While Eulerian diagnostics quantify local velocity agreement, they do not necessarily assess whether a velocity field reproduces realistic transport pathways. In ocean transport problems, relatively small velocity differences can accumulate over time and generate large deviations in particle trajectories. This limitation is particularly relevant in the Arctic Ocean, where freshwater redistribution, connectivity, and export pathways depend on cumulative transport processes rather than on instantaneous velocity agreement alone.

In a Lagrangian framework, the motion of a passive particle advected by a velocity field is governed by

$$\frac{d\mathbf{x}}{dt} = \mathbf{v}(\mathbf{x}, t), \tag{1}$$

where $\mathbf{x}(t)$ denotes the particle position and $\mathbf{v}(\mathbf{x}, t)$ is the velocity field provided by the product under evaluation. By integrating this equation forward in time, synthetic trajectories can be generated and compared with observed drifter trajectories.

Transport pathways in ocean flows described by Eq. (1) have often been interpreted using Lagrangian Coherent Structures (LCSs) (Shadden et al., 2009; Mendoza et al., 2014; García-Sánchez et al., 2022a). These dynamically invariant structures organize fluid particle motion by partitioning the ocean surface into regions with distinct particle evolution and by identifying

https://doi.org/10.5194/egusphere-2026-3629
Preprint. Discussion started: 26 June 2026

transport barriers that separate them. As a result, they provide a more robust description of transport dynamics than individual trajectories alone.

In the present work to identify these LCSs, we use the Lagrangian descriptor M (Mancho et al., 2013), defined for an initial condition $\mathbf{x}_0$ at time t_0 over an integration time τ as

$$M(\mathbf{x}_0, t_0, \tau) = \int_{t_0-\tau}^{t_0+\tau} \|\mathbf{v}(\mathbf{x}(\mathbf{x}_0, t), t)\| \, dt, \tag{2}$$

where $\mathbf{x}(\mathbf{x}_0, t)$ is the trajectory starting from $\mathbf{x}_0$. Thus, M measures the arc-length of the trajectory over the selected time interval. Sharp gradients in the spatial distribution of M reveal the LCSs organizing the flow. Forward-time integration highlights structures associated with the stable manifolds of hyperbolic trajectories, whereas backward-time integration highlights structures associated with their unstable manifolds.

To complement the Eulerian analysis, we implemented a Lagrangian validation based on the Lagrangian Uncertainty Quantification (LUQ) framework described in (García-Sánchez et al., 2025, 2021, 2022b, 2023). In contrast to Eulerian comparisons, and to other Lagrangian validation approaches (Vastano and Barron, 1994; Barron et al., 2007; Liu and Weisberg, 2011), LUQ evaluates the ability of surface current products to reproduce the observed evolution of drifting particles while accounting for the underlying transport geometry of the flow.

A key result underlying the LUQ framework is that transport deviations are not randomly distributed. Instead, they exhibit coherent spatial patterns that are closely related to the LCSs revealed by the Lagrangian descriptor M. This similarity reflects the fact that the coherent transport structures governing particle motion also organize the spatial distribution of transport deviations. In particular, regions separated by transport barriers may exhibit markedly different transport outcomes and transport deviations, reflecting the dynamical organization of the flow.

The LUQ methodology evaluates product performance by comparing observed drifter trajectories with trajectories obtained by advecting particles using the velocity field under evaluation. Consider two observed drifter positions $\mathbf{p}_0$ and $\mathbf{p}^*$, corresponding to times t_0 and $t^* = t_0 + \tau$, respectively. Starting from an initial position $\mathbf{x}_0$ in a neighbourhood of $\mathbf{p}_0$, i.e. $\mathbf{x}_0 \in X_0(\mathbf{p}_0, R)$, a simulated trajectory is obtained by integrating the velocity field forward in time. The corresponding L_{UQ} metric is defined as

$$L_{UQ}(\mathbf{x}_0, t_0, \tau; \mathbf{p}^*) = \|\mathbf{x}^* - \mathbf{p}^*\| . \tag{3}$$

where $\mathbf{x}^*$ denotes the simulated particle position at time t^*. Thus, L_{UQ} measures the distance between the simulated and observed particle positions at the verification time. In the present application, the norm is computed as the geodesic distance on the Earth's surface, so that L_{UQ} is expressed in kilometres. Larger values indicate poorer agreement between observed and simulated transport pathways.

A single trajectory-to-trajectory comparison may be misleading because transport is strongly affected by nearby dynamical barriers and sensitivity to initial conditions. Small perturbations in the initial position may lead to substantially different trajectory outcomes, especially in regions characterized by mesoscale variability, strong shear, or recirculating flows. For this

https://doi.org/10.5194/egusphere-2026-3629
Preprint. Discussion started: 26 June 2026

reason, L_{UQ} is evaluated not only at the observed initial position, but over a neighborhood $\mathbf{X}_0(\mathbf{p}_0, r)$ surrounding it. The spatially averaged metric is defined as:

$$\overline{L_{UQ}}(t_0, \tau; \mathbf{p}^*, R) = \frac{1}{|\mathbf{X}_0(\mathbf{p}_0, R)|} \int_{\mathbf{X}_0(\mathbf{p}_0, R)} L_{UQ}(\mathbf{x}_0, t_0, \tau; \mathbf{p}^*)\, d\mathbf{x}_0. \tag{4}$$

To further reduce the dependence on the specific choice of the initial time t_0, a temporal average over an interval T may also be considered:

$$[\overline{L_{UQ}}](\tau; \mathbf{p}^*, R; t_{st}, T) = \frac{1}{T} \int_{t_{st}}^{t_{st}+T} \overline{L_{UQ}}(t_0, \tau; \mathbf{p}^*, R)\, dt_0. \tag{5}$$

The spatial and temporal averaging procedures reduce the sensitivity of the validation to small-scale variability and trajectory divergence, providing a more robust assessment of transport consistency between observations and modelled velocity fields. At the same time, the connection between the resulting L_{UQ} fields and the LCSs revealed by M provides a dynamical interpretation of the validation results.

In García-Sánchez et al. (2025), the temporal average in Eq. (5) was used to obtain a representative measure of the capability of a velocity dataset to reproduce Lagrangian transport over a given time interval. In the present work, we adopt a complementary approach to characterize the temporal distribution of the spatially averaged L_{UQ} values, $\overline{L_{UQ}}(t_0, \tau; \mathbf{p}^*, R)$, over all available initial times t_0. Rather than reducing the information to a single average value, these distributions are represented using boxplots, which provide a robust measure of the central tendency jointly with information on temporal variability and dispersion. This representation highlights differences in both the typical performance and the consistency of the various surface current products to be assessed across the different oceanographic regimes considered in this study.

To assess the robustness of the LUQ diagnostics to the choice of methodological parameters, we performed a sensitivity analysis using different integration time scales τ and neighbourhood size R. This analysis supported the use of $\tau = 5$ days and $R = 10$ km. The choice of $\tau = 5$ days represents a compromise between resolving short-term transport divergence and avoiding excessive trajectory dispersion over longer integration periods. The choice of $R = 10$ km provides a neighbourhood sufficiently large to capture uncertainty around the drifter position arising from nearby dynamical structures associated with the underlying flow, while remaining small relative to the spatial scales explored by the drifter over the integration period τ. In particular, this size is substantially smaller than the distances travelled by the drifters considered in this approach over five days, with mean regional displacements typically ranging between 30 and 133 km, depending on the case study. This configuration was therefore used for all LUQ diagnostics presented in the following sections, providing a consistent framework for comparing products across contrasting Arctic circulation regimes.

3.4 Case studies

To evaluate the capability of the different surface current products to reproduce transport pathways under contrasting dynamical regimes, nine representative drifter trajectories were selected across the Arctic and adjacent sub-Arctic regions (Fig. 3). These

https://doi.org/10.5194/egusphere-2026-3629
Preprint. Discussion started: 26 June 2026

cases include major Arctic gateways, boundary currents, recirculating gyres, shelf inflow regions, and subpolar current systems, providing a broad framework for testing product performance under different dynamical conditions.

The selected Arctic and gateway cases include the Bering Strait (BST), which captures the inflow of Pacific-origin waters into the Arctic Ocean; the West Spitsbergen Current (WSC) and Barents Sea Opening (BSO), which represent Atlantic Water inflow pathways into the Arctic; the East Greenland Current (EGC), a narrow and energetic boundary current associated with southward freshwater and sea-ice export; the Beaufort Gyre (BEA), a wind-driven anticyclonic circulation regime characterized by freshwater accumulation and strong upper-ocean stratification; and the Transpolar Drift (TPD), which represents a major pathway for trans-Arctic drift and export.

Additional sub-Arctic and North Atlantic cases include the Lofoten Gyre (LFG), a quasi-permanent mesoscale recirculation in the Nordic Seas; the Labrador Current (LBC), a western boundary current linked to freshwater export from the Arctic and subpolar seas; and the Gulf Stream (GST), an energetic western boundary current included as a dynamically contrasting benchmark outside the Arctic proper.

Together, these case studies span a wide range of transport regimes, from relatively coherent boundary currents to strongly recirculating and mesoscale-dominated flows. They are therefore suitable for assessing whether Eulerian agreement with drifter velocities translates into realistic Lagrangian transport pathways.

Figure 3 shows the trajectories of the selected drifters over the corresponding evaluation periods, and Table 1 summarizes their temporal windows and characteristic trajectory lengths. Because the selected cases operate over different spatial and temporal scales, the Lagrangian metrics are presented in normalized form. Specifically, the L_{UQ} metric is normalized by L, defined as the maximum distance traveled by each drifter during the evaluation period and reported in Table 1. This normalization allows direct comparison between case studies independently of their characteristic transport scale.

Table 1. Summary of the drifter case studies, including case-study identifiers, evaluation period (start and end date), trajectory duration (number of days), and drifter trajectory length L (total kilometers travelled by the drifter during the case study).

Case Study	ID	Start date	End date	Days	L (km)
Bering Strait	BST	04-10-2016	03-11-2016	30	893.67
Lofoten Gyre	LFG	09-09-2021	09-10-2021	30	597.81
West Spitsbergen Current	WSC	18-11-2016	18-12-2016	30	615.85
East Greenland Current	EGC	30-05-2017	29-07-2017	60	1008.13
Barents Sea Opening	BSO	09-12-2016	07-02-2017	60	716.98
Beaufort Gyre	BEA	01-09-2020	31-10-2020	60	967.66
Gulf Stream	GST	24-05-2016	21-10-2016	150	1922.43
Labrador Current	LBC	28-08-2015	25-01-2016	150	2326.25
Transpolar Drift	TPD	24-10-2018	23-03-2019	150	1080.75

https://doi.org/10.5194/egusphere-2026-3629
Preprint. Discussion started: 26 June 2026

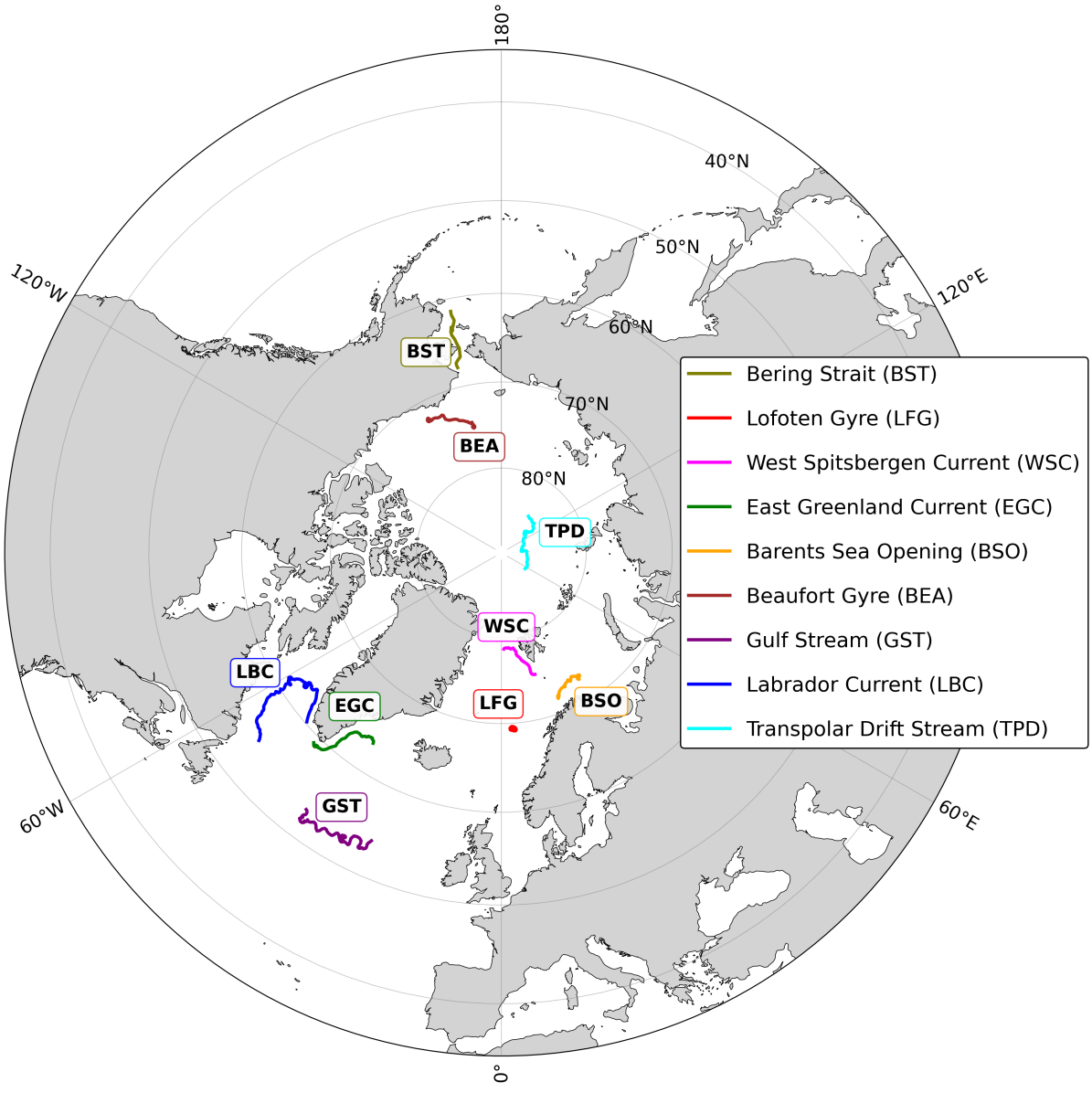

Figure 3. Pan-Arctic and sub-Arctic map showing the selected drifter trajectories used for the Lagrangian evaluation. Each trajectory corresponds to a dynamically distinct case study, including Arctic gateways, boundary currents, recirculating gyres, shelf inflow regions, and subpolar current systems. Case-study abbreviations are shown on the map and summarized in Table 1.

https://doi.org/10.5194/egusphere-2026-3629
Preprint. Discussion started: 26 June 2026

4 Results

4.1 Surface current product comparison

Figure 4 compares the probability density distributions of current speed from the evaluated products and the drifter observations. The distributions provide a first-order assessment of whether each product reproduces the observed range and frequency of near-surface current intensities sampled by the drifters.

NeurOST and OSCAR reproduce the observed distribution most consistently, particularly for moderate current speeds. GlobCurrent shows a similar mean speed to the drifters but a smoother distribution, suggesting that the combination of geostrophic and Ekman components may reduce part of the observed small-scale variability. GLORYS and TOPAZ capture the broad range of observed velocities but tend to smooth the highest-speed tail, while AVISO clearly underestimates the occurrence of energetic currents.

The reduced high-speed tail in AVISO is consistent with the fact that it represents only the geostrophic component of the surface circulation and does not explicitly include wind-driven, inertial, or other ageostrophic motions sampled by the drifters. More generally, differences among the distributions reflect both product-specific dynamical content and the different effective depths represented by each dataset.

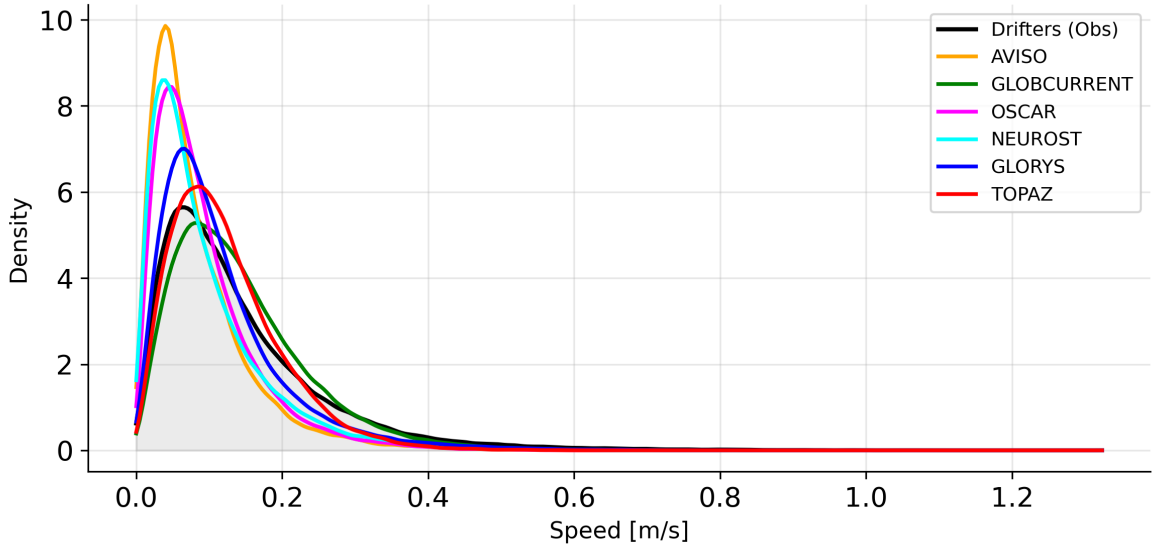

Figure 4. Probability density distributions of current speed from drifter observations and evaluated surface current products. The black solid line and light gray shading represent the drifter-observed distribution. Product distributions are color-coded as follows: AVISO (orange), GlobCurrent (green), OSCAR (magenta), NeurOST (cyan), GLORYS (blue), and TOPAZ (red). The horizontal axis denotes current speed (m s^{-1}), and the vertical axis indicates probability density.

https://doi.org/10.5194/egusphere-2026-3629
Preprint. Discussion started: 26 June 2026

4.2 Eulerian evaluation of Arctic surface current products

The six surface current products were evaluated against drifter-derived near-surface velocities using classical Eulerian diagnostics, including root-mean-square error (RMSE), bias, correlation, current speed distributions, and directional statistics. The comparison includes products representing distinct dynamical components of the Arctic circulation: geostrophic currents derived from satellite altimetry, machine-learning reconstructions of geostrophic currents, total or mixed-layer surface current products, and ocean reanalyses.

Metrics were computed over the common Arctic domain and collocated in space and time with available drifter observations. Because the evaluated products differ in their dynamical content and effective sampling depth, the statistics should be interpreted as an assessment of their ability to reproduce the near-surface motion sampled by drogued drifters, rather than as a strict comparison of identical physical quantities.

Figure 5 summarizes the overall performance of the different products using a Taylor diagram. NeurOST and OSCAR exhibit the best overall agreement with drifter observations, combining relatively high correlations with reduced dispersion errors. The good performance of NeurOST suggests that the machine-learning reconstruction of SSH and geostrophic currents constrained by altimetry and SST can improve the representation of mesoscale surface circulation relative to conventional altimetric mapping. The performance of OSCAR reflects the added value of explicitly including mixed-layer and wind-driven contributions, which are partly sampled by drogued drifters.

GlobCurrent and GLORYS show intermediate performance. GlobCurrent reproduces the mean observed current speed particularly well, consistent with its use of total currents at a depth comparable to the drifter drogue depth, although its distribution is smoother than the drifter observations. GLORYS captures part of the large-scale circulation variability but also tends to smooth near-surface velocity extremes.

AVISO and TOPAZ show weaker agreement in current speed relative to the best-performing products. For AVISO, this is consistent with its purely geostrophic formulation, which does not explicitly include wind-driven, inertial, or other ageostrophic contributions sampled by drifters. TOPAZ captures part of the component-wise flow variability, but its near-surface speed agreement is lower than that of NeurOST, OSCAR, GlobCurrent, and GLORYS in the global Eulerian statistics.

All products exhibit a marked seasonal cycle in Eulerian skill, with generally improved agreement during summer and reduced skill during winter and early spring (Fig. 6). This seasonal behavior reflects the combined influence of changing sea-ice cover, variable observational sampling, seasonal wind forcing, and the uneven availability of drifter observations across the Arctic.

NeurOST and OSCAR generally provide the lowest RMSE values and highest correlations throughout most of the year. Their improved performance likely reflects the use of additional dynamical or observational information beyond conventional altimetric mapping: SST-constrained reconstruction in NeurOST and mixed-layer, wind-driven contributions in OSCAR. GlobCurrent and GLORYS show intermediate skill, whereas AVISO exhibits larger errors and lower correlations, particularly during autumn and winter.

https://doi.org/10.5194/egusphere-2026-3629
Preprint. Discussion started: 26 June 2026

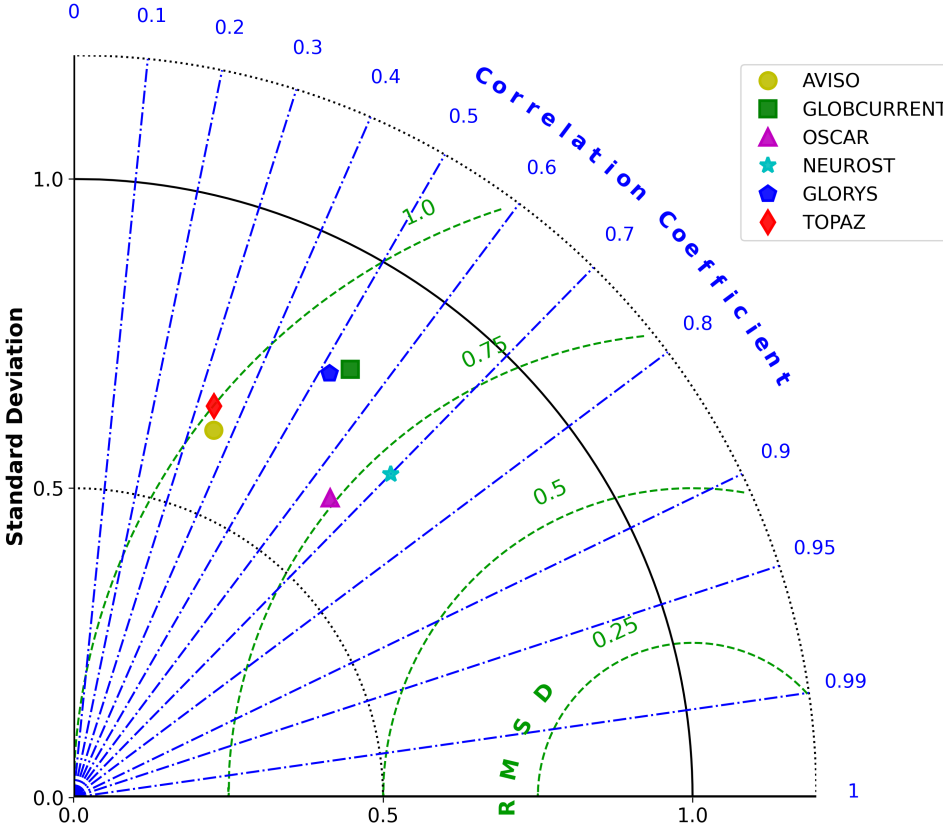

Figure 5. Taylor diagram summarizing the statistical skill of surface current products relative to drifter observations. The diagram displays the correlation coefficient, the root-mean-square difference (RMSD), and the standard deviation. Product performance is represented by distinct marker-color combinations: AVISO (orange circle), GlobCurrent (green square), OSCAR (magenta triangle), NeurOST (cyan star), GLORYS (blue pentagon), and TOPAZ (red diamond). NeurOST and OSCAR show the highest overall statistical skill, whereas AVISO and TOPAZ show weaker agreement in current speed relative to the drifter observations.

https://doi.org/10.5194/egusphere-2026-3629
Preprint. Discussion started: 26 June 2026

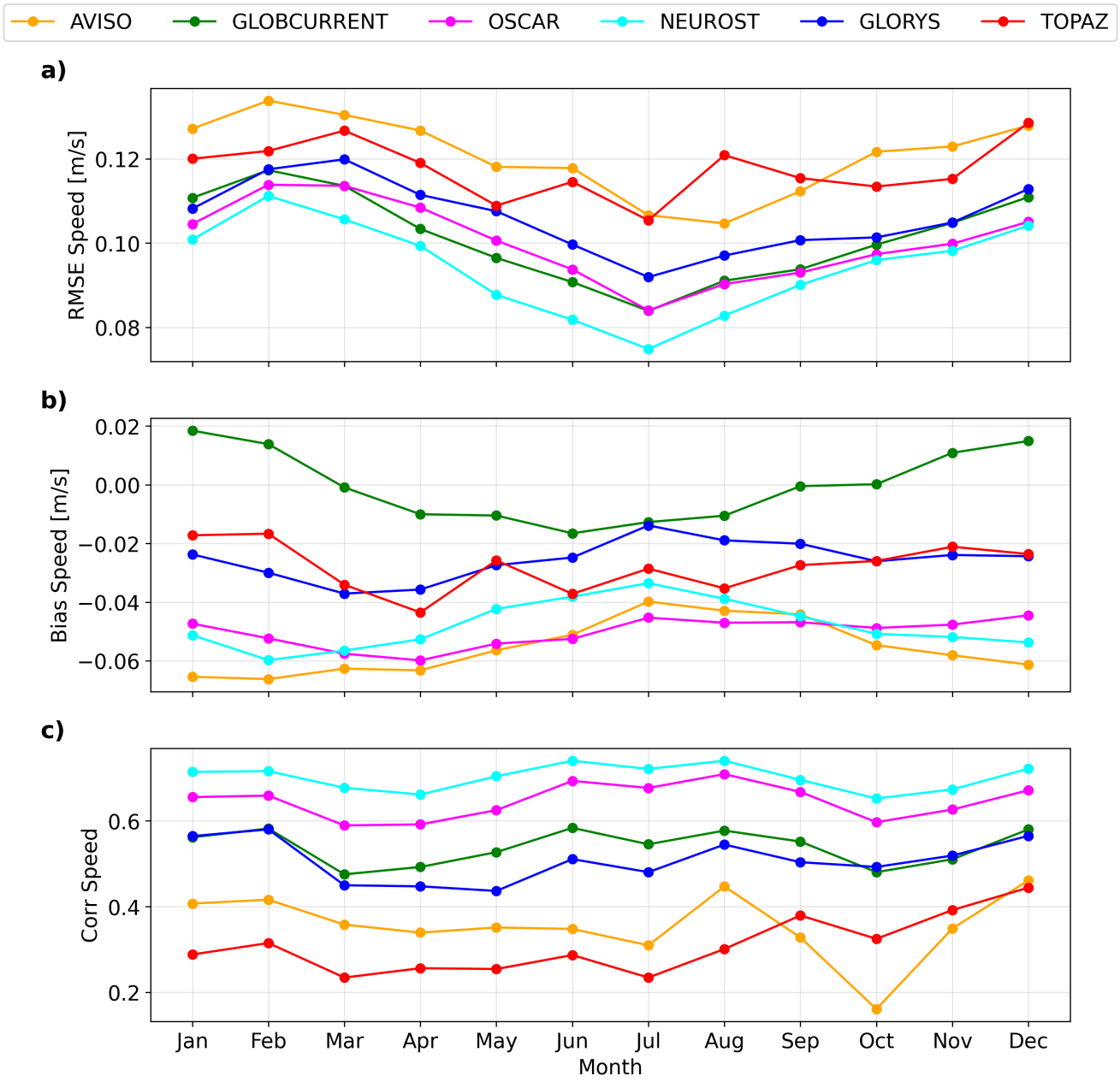

Figure 6. Monthly evolution of Eulerian validation metrics for the different surface current products relative to drifter observations: a) root-mean-square error (RMSE), b) bias, and c) correlation. Product colors are as follows: AVISO (orange), GlobCurrent (green), OSCAR (magenta), NeurOST (cyan), GLORYS (blue), and TOPAZ (red). Metrics show a marked seasonal dependence, with generally improved agreement during summer and reduced skill during winter and early spring.

https://doi.org/10.5194/egusphere-2026-3629
Preprint. Discussion started: 26 June 2026

Table 2. Statistical metrics comparing model outputs with drifter observations for the zonal velocity component (U), meridional velocity component (V), current speed, and vector velocity (U+V). Reported metrics include the number of paired observations (N), mean observed value (Mean Obs), mean modeled value (Mean Mod), bias, standard deviation of the error (STD Error), root-mean-square error (RMSE), Pearson correlation coefficient (Corr), and skill score. Best performing products are highlighted in bold green, and worst performing products are indicated in bold red for each statistical metric.

MODEL	N	Mean Obs	Mean Mod	Bias	STD Error	RMSE	Corr	Skill Score
u-component								
AVISO	98,113	-0.002	-0.010	**-0.008**	**0.125**	**0.125**	**0.329**	**0.018**
GLOBCURRENT	105,457	-0.003	0.001	0.004	0.104	0.104	0.667	0.373
GLORYS	109,904	-0.004	0.001	0.004	0.109	0.110	0.588	0.294
NEUROST	103,764	-0.003	-0.005	**-0.002**	**0.086**	**0.086**	**0.756**	**0.569**
OSCAR	104,036	-0.003	-0.005	-0.003	0.092	0.092	0.714	0.498
TOPAZ	69,780	0.003	0.008	0.005	0.124	0.124	0.473	0.135
v-component								
AVISO	98,113	0.003	0.007	0.003	**0.126**	**0.126**	**0.291**	**-0.029**
GLOBCURRENT	105,457	0.003	-0.002	-0.005	0.104	0.104	0.647	0.337
GLORYS	109,904	0.003	0.001	-0.002	0.110	0.110	0.561	0.250
NEUROST	103,764	0.003	0.007	0.004	**0.087**	**0.087**	**0.733**	**0.532**
OSCAR	104,036	0.003	0.003	**0.000**	0.089	0.089	0.718	0.514
TOPAZ	69,780	0.003	-0.005	**-0.009**	0.125	0.125	0.469	0.133
Speed								
AVISO	98,113	0.139	0.085	**-0.054**	0.107	**0.120**	0.356	**-0.214**
GLOBCURRENT	105,457	0.143	0.143	**0.000**	0.101	0.101	0.542	0.219
GLORYS	109,904	0.142	0.117	-0.025	0.102	0.105	0.517	0.141
NEUROST	103,764	0.143	0.095	-0.048	**0.081**	**0.094**	**0.700**	**0.316**
OSCAR	104,036	0.143	0.093	-0.050	0.086	0.100	0.650	0.233
TOPAZ	69,780	0.151	0.123	-0.028	**0.114**	0.117	**0.338**	-0.052

Vector velocity (U+V)		
Model	N	RMSE
AVISO	98,113	**0.178**
GLOBCURRENT	105,457	0.147
GLORYS	109,904	0.155
NEUROST	103,764	**0.122**
OSCAR	104,036	0.128
TOPAZ	69,780	0.176

Most products exhibit predominantly negative biases, indicating a general tendency to underestimate near-surface current intensity relative to drifter observations. This underestimation is particularly evident for products that smooth high-frequency or ageostrophic variability, including purely geostrophic altimetric estimates and some reanalysis or combined products.

The seasonal aggregation of the Eulerian metrics (Fig. 7) confirms the monthly patterns while highlighting systematic differences among products. Summer exhibits the highest correlations and lowest RMSE values for most products, consistent with reduced sea-ice extent, improved observational constraints, and more favorable drifter sampling.

NeurOST and OSCAR maintain the best overall seasonal performance, particularly during summer and autumn. The comparatively better agreement of these products suggests that incorporating additional observational constraints, mixed-layer

https://doi.org/10.5194/egusphere-2026-3629
Preprint. Discussion started: 26 June 2026

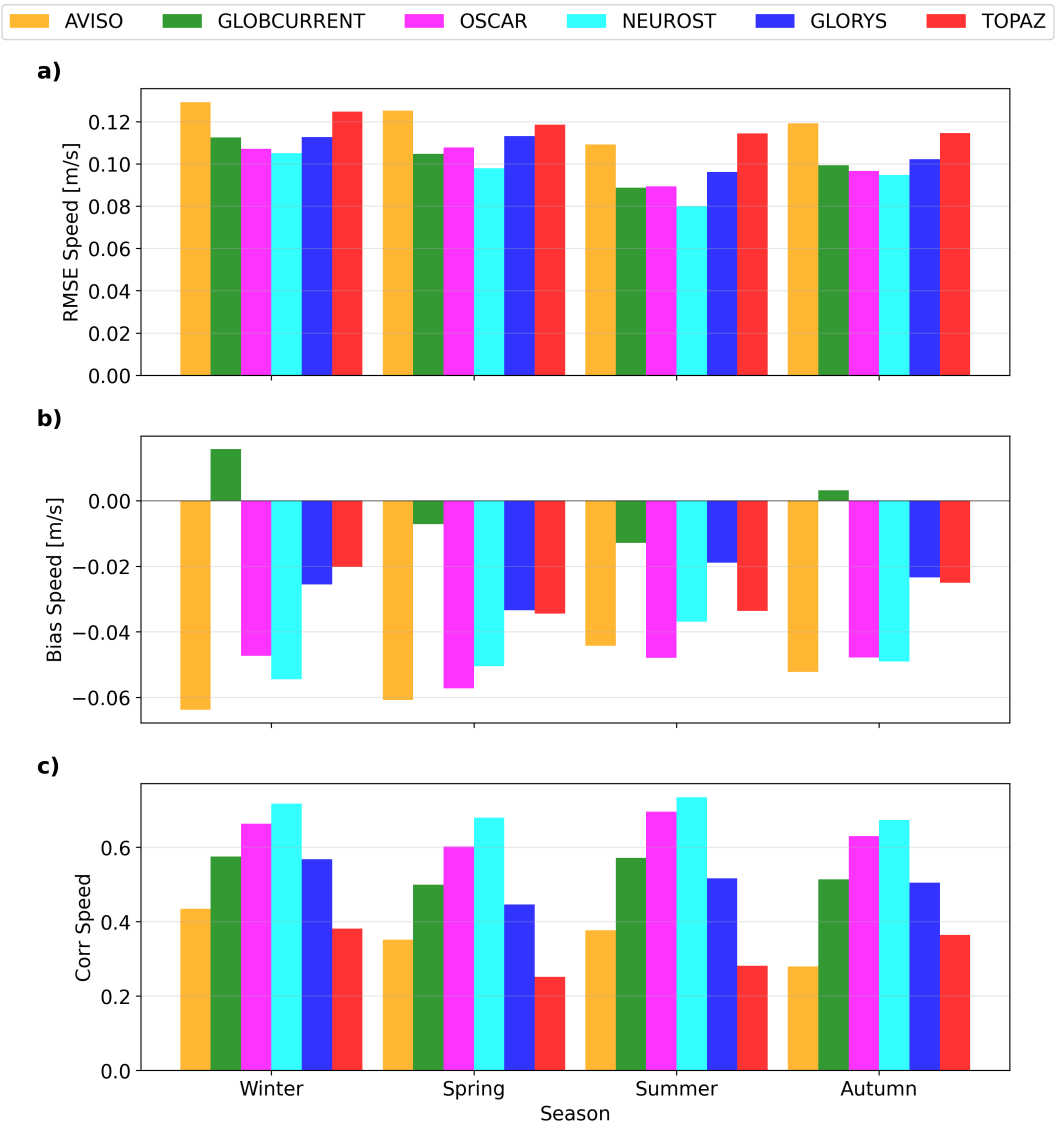

Figure 7. Seasonal Eulerian validation metrics relative to drifter-derived velocities: a) root-mean-square error (RMSE), b) bias, and c) correlation. Product colors are as follows: AVISO (orange), GlobCurrent (green), OSCAR (magenta), NeurOST (cyan), GLORYS (blue), and TOPAZ (red). Most products show improved agreement during summer, while winter and spring exhibit lower correlations and larger errors associated with sea-ice cover, reduced observational sampling, and enhanced near-surface dynamical variability.

https://doi.org/10.5194/egusphere-2026-3629
Preprint. Discussion started: 26 June 2026

dynamics, or wind-driven contributions improves the representation of Arctic near-surface transport variability beyond what can be captured by conventional altimetry-only geostrophic currents.

Seasonal differences are especially pronounced during winter and spring, when sea-ice cover, reduced satellite sampling, stronger wind-driven variability, and limited drifter coverage introduce larger uncertainties in surface current estimation. These conditions particularly affect products that rely strongly on satellite observations or that do not explicitly represent ageostrophic near-surface dynamics.

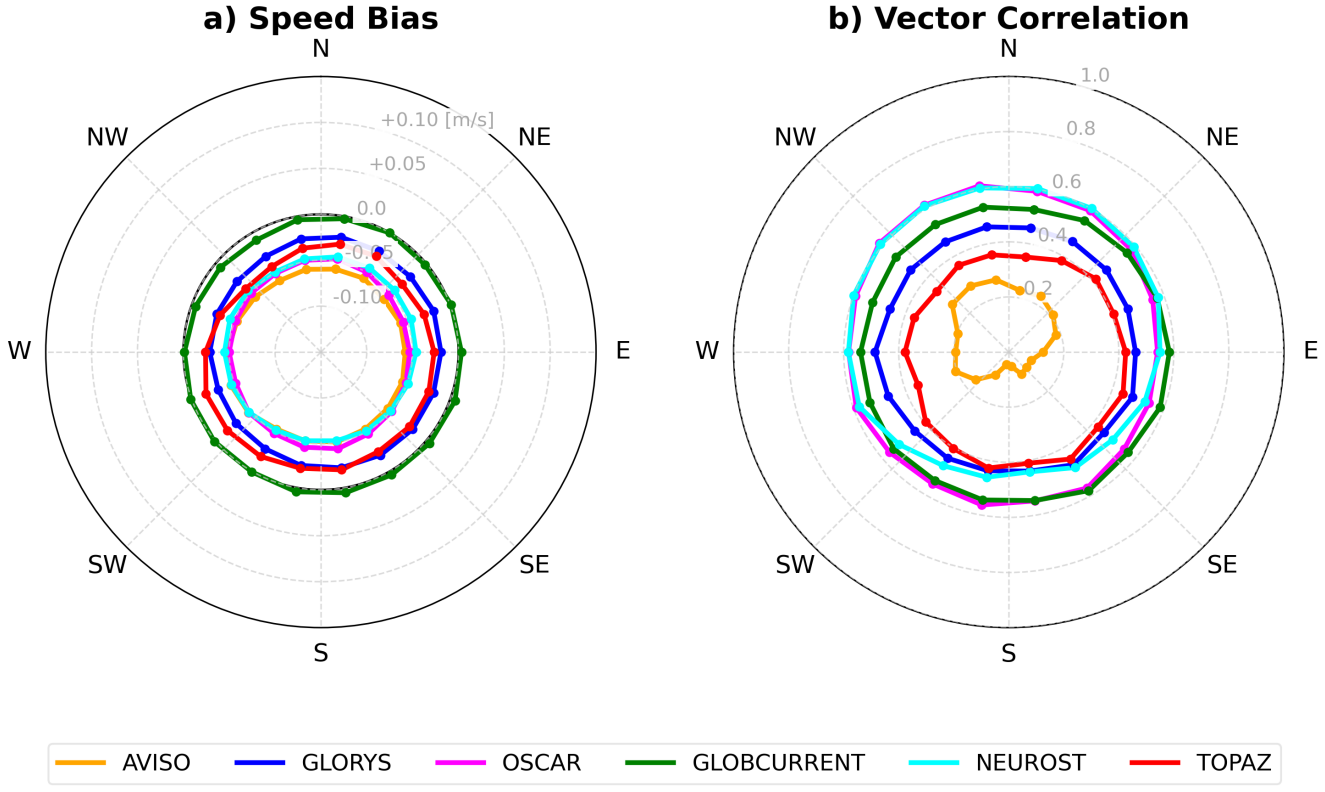

Figure 8. Directional performance of the evaluated surface current products relative to drifter observations. (a) Mean current speed bias (m s^{-1}) as a function of observed flow direction, where positive values indicate product overestimation and negative values indicate underestimation. (b) Vector correlation coefficient between product-derived and observed currents for each directional sector.

Directional statistics are presented in Fig. 8. These diagnostics assess whether the products reproduce not only the magnitude of the observed currents, but also their preferred directions. Most products capture the dominant flow orientations sampled by the drifters, including directions associated with boundary currents and gyre circulation. However, differences emerge in both speed bias and vector correlation as a function of flow direction.

NeurOST and OSCAR show the strongest directional agreement overall, consistent with their higher Eulerian skill in the global statistics. AVISO exhibits larger directional discrepancies and weaker vector correlations, reflecting the limitations of

https://doi.org/10.5194/egusphere-2026-3629
Preprint. Discussion started: 26 June 2026

purely geostrophic altimetric currents in regions where wind-driven, inertial, or mixed-layer processes contribute substantially to the observed drifter motion. GlobCurrent, GLORYS, and TOPAZ show intermediate behavior, with performance depending on direction and regional sampling.

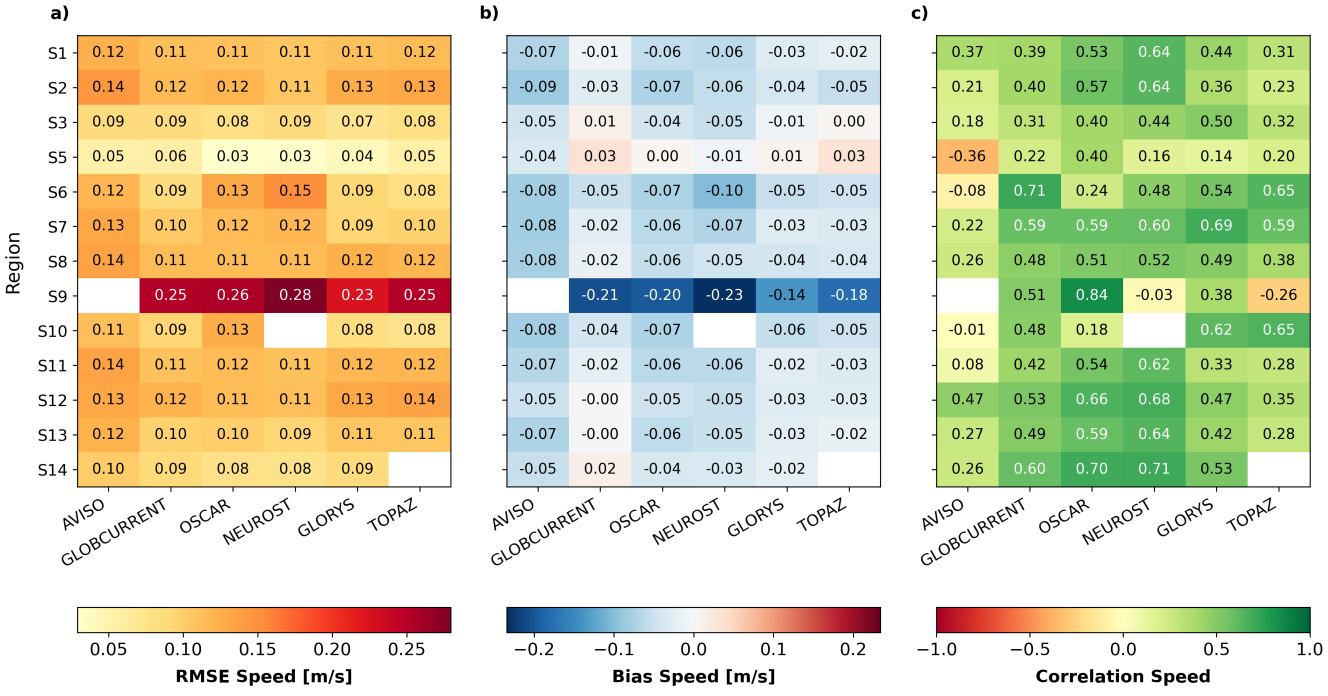

Figure 9. Regional Eulerian validation metrics for the evaluated surface current products relative to drifter observations. Panels show (a) RMSE, (b) bias, and (c) correlation for the Arctic regions defined in Fig. 2. Product performance exhibits strong regional variability, with reduced skill in dynamically complex regions such as shallow shelves, inflow regions, and narrow Arctic gateways.

Regional statistics reveal strong spatial variability in product performance (Fig. 9). The best agreement is generally obtained in regions where the large-scale circulation is relatively coherent and where drifter sampling is more favorable. In contrast, reduced skill is found in dynamically complex regions such as shallow shelves, Pacific and Atlantic inflow pathways, and narrow Arctic gateways.

These regions are characterized by strong bathymetric steering, intensified mesoscale variability, ice-ocean interactions, and enhanced ageostrophic dynamics. Such processes are difficult to capture consistently across products, particularly for datasets that rely primarily on geostrophic balance or that have limited effective resolution near coastlines and gateways.

The regional degradation observed for AVISO further highlights the limitations of altimetry-only geostrophic currents in reproducing Arctic near-surface transport variability. Products incorporating additional observational constraints, wind-driven components, mixed-layer dynamics, or model-based circulation tend to perform better in several regions, although no single product performs uniformly best across the full Arctic domain.

https://doi.org/10.5194/egusphere-2026-3629
Preprint. Discussion started: 26 June 2026

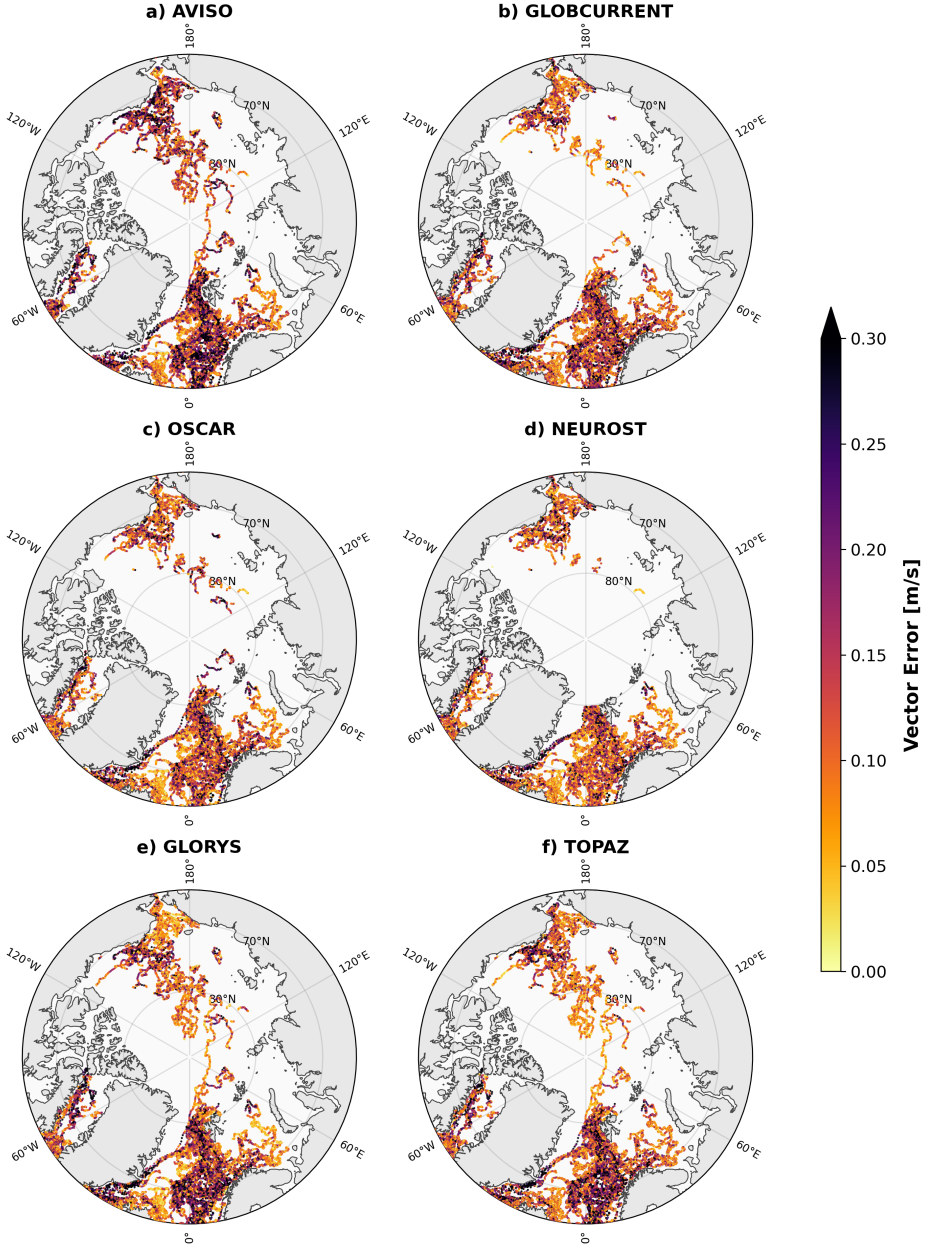

Figure 10. Spatial distribution of vector velocity error for the evaluated surface current products relative to drifter observations. Panels show the error magnitude (m s^{-1}) along drifter trajectories for AVISO, GlobCurrent, OSCAR, NeurOST, GLORYS, and TOPAZ. The color scale is saturated at 0.3 m s^{-1} to emphasize regional differences and highlight localized areas of enhanced product–drifter mismatch.

https://doi.org/10.5194/egusphere-2026-3629
Preprint. Discussion started: 26 June 2026

To complement the aggregated regional statistics, a track-by-track spatial visualization of the errors provides a more detailed view of where product deviations occur along the observed drifter trajectories.

Figure 10 shows the spatial distribution of the vector velocity error for each product. The largest errors are concentrated along dynamically energetic regions, including the Nordic Seas, the Barents Sea slope, boundary-current systems, and narrow gateway regions. These areas are characterized by strong topographic steering, mesoscale variability, and sharp current gradients, making them particularly challenging for gridded current products.

Products with broader spatial coverage, such as AVISO, GLORYS, and TOPAZ, provide more continuous error maps across the Arctic domain, whereas products affected by sea-ice masking or observational constraints show more fragmented coverage in ice-covered regions. Despite these coverage differences, the spatial patterns consistently indicate enhanced errors in regions where small spatial displacements of boundary currents or recirculating structures can generate large point-wise velocity discrepancies.

Figure 11 shows the corresponding speed bias, defined as product minus drifter speed. Most products exhibit a tendency toward negative bias over large parts of the domain, indicating an underestimation of near-surface current intensity relative to the drifter observations. This underestimation is consistent with the smoothing of high-frequency variability, unresolved ageostrophic motions, and limitations in representing narrow or rapidly varying currents.

Localized positive biases are also observed near steep topographic features and gateway regions, indicating that some products may overestimate current speed where boundary flows are displaced, overly intensified, or not correctly phased relative to the drifter trajectories. Overall, the spatial error and bias patterns highlight that product performance is strongly regime-dependent and that the main discrepancies occur in regions of strong dynamical gradients and complex ice-ocean interactions.

Overall, the Eulerian analysis shows that products incorporating additional observational constraints, wind-driven contributions, or mixed-layer dynamics generally outperform conventional altimetry-only geostrophic currents in reproducing drifter-derived near-surface velocities. However, product skill varies strongly by season and region, and no single product performs uniformly best across all Arctic circulation regimes. These results motivate the complementary Lagrangian analysis presented in the next section, which evaluates whether local velocity agreement translates into realistic transport pathways.

4.3 Lagrangian validation of Arctic transport pathways

While the Eulerian analysis provides information on local velocity agreement, it does not directly evaluate the capability of the different products to reproduce realistic transport pathways. To address this limitation, the surface current products were further assessed using a Lagrangian validation based on the Lagrangian Uncertainty Quantification (LUQ) framework described in Sect. 3.3. Unlike conventional trajectory-based comparisons, LUQ quantifies transport deviations between observed (ground-truth) and synthetic trajectories while accounting for their organization by the underlying transport structures of the flow. In this framework, uncertainty is defined through these transport deviations and is interpreted as a spatially organized field. Rather than evolving as a random diffusive cloud around the ground-truth trajectory, transport deviations are organized by the transport geometry of the underlying velocity field and by the Lagrangian coherent structures governing particle evolution.

https://doi.org/10.5194/egusphere-2026-3629
Preprint. Discussion started: 26 June 2026

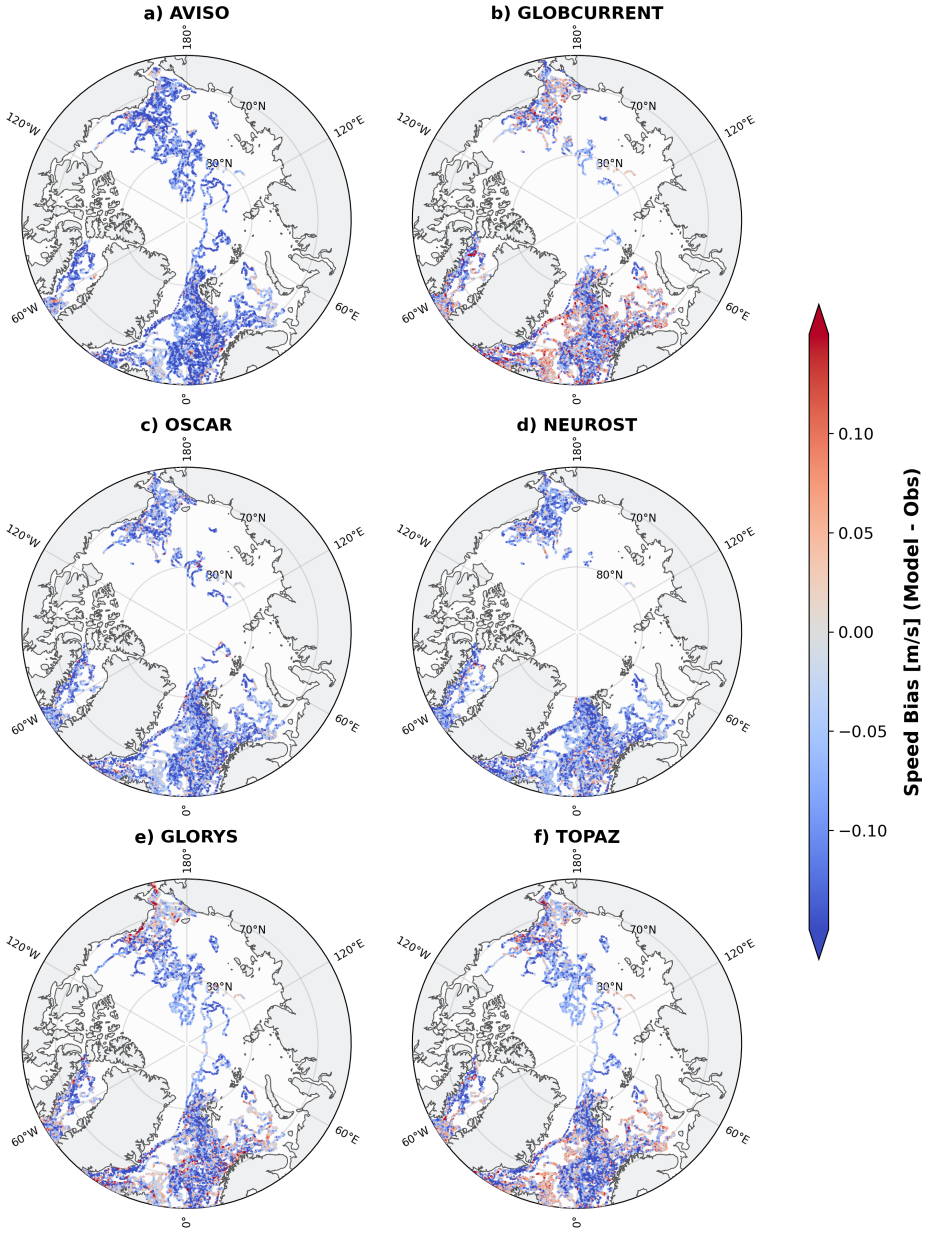

Figure 11. Spatial distribution of current speed bias for the evaluated surface current products relative to drifter observations. Bias is defined as product speed minus drifter speed, so negative values indicate underestimation and positive values indicate overestimation. Panels show AVISO, GlobCurrent, OSCAR, NeurOST, GLORYS, and TOPAZ. The diverging color scale highlights regions of localized underestimation and overestimation across the Arctic and sub-Arctic domain.

https://doi.org/10.5194/egusphere-2026-3629
Preprint. Discussion started: 26 June 2026

The Lagrangian analysis is based on the nine drifter case studies introduced in Sect. 3.4. These cases span contrasting transport regimes, including Arctic gateways, Atlantic and Pacific inflow pathways, freshwater export currents, recirculating gyres, shelf-influenced flows, and energetic subpolar boundary currents. This selection allows the products to be evaluated under a broad range of dynamical conditions, from relatively coherent boundary-current systems to highly variable and mesoscale-dominated regimes. For each case study, synthetic trajectories were generated from initial conditions distributed within a square neighbourhood of size R of the drifter position, advected using the different velocity products, and subsequently compared with the observed drifter trajectories. In contrast to the Eulerian framework, which evaluates local velocity differences, the Lagrangian analysis assesses how these differences accumulate over time and affect the representation of transport pathways, retention, and connectivity. The resulting L_{UQ} fields provide information not only on the magnitude of transport deviations but also on their spatial organization around the observed trajectory.

To better understand the dynamical origin of these differences, we first examine two representative cases using the Lagrangian descriptor M together with the corresponding L_{UQ} fields. These diagnostics provide a process-oriented interpretation of trajectory errors by linking them to the spatial organization of the velocity field and to the presence of transport barriers, recirculation regions, and export pathways.

The Lofoten Gyre provides an illustrative example of the dynamical interpretation of the LUQ framework. In this mesoscale recirculation regime, particle evolution is controlled not only by current intensity but also by the position of the vortex core and the surrounding transport barriers identified by the Lagrangian descriptor. The corresponding L_{UQ} fields shown in Fig. 12 reveal that transport deviations are themselves structured within the neighbourhood considered. Links between the spatial organization of L_{UQ} and the underlying LCSs have been established in previous studies (García-Sánchez et al., 2021, 2022b, 2023, 2025). In the present application, the L_{UQ} fields are evaluated only over a small neighbourhood surrounding the observed drifter position, which is sufficient for the product-validation problem addressed here. Although extending the computational domain would reveal the larger-scale L_{UQ} patterns whose spatial organization resembles that of the underlying LCS network, the local domain adopted here captures the transport variability most relevant for the validation of surface current products. The coexistence of lower and higher L_{UQ} values within the neighbourhood reflect the local transport organization and sensitivity to nearby initial conditions induced by the underlying flow structures. Averaging over this neighbourhood, therefore, accounts for the range of dynamically plausible transport pathways around the observed drifter position, rather than relying on a single initial condition. Accordingly, transport deviations are not uniformly distributed around the observed drifter position, but are organized by the underlying recirculation and its associated transport barriers. Products that place the recirculating structure closer to that experienced by the observed drifter produce lower L_{UQ} values, because particles initialized within the neighbourhood remain closer to the observed trajectory throughout their evolution. In contrast, products that shift the vortex core, smooth the transport barriers, or place the drifter neighbourhood near the edge of a different recirculation structure lead to rapid divergence from the observed pathway after only $\tau = 5$ days.

This case demonstrates that the largest Lagrangian errors are not necessarily caused by large local velocity errors alone. Instead, they can arise from relatively small spatial shifts in the transport topology. In mesoscale-dominated regimes such as the Lofoten Gyre, a modest displacement of the vortex core can determine whether particles remain trapped, circulate locally, or

https://doi.org/10.5194/egusphere-2026-3629
Preprint. Discussion started: 26 June 2026

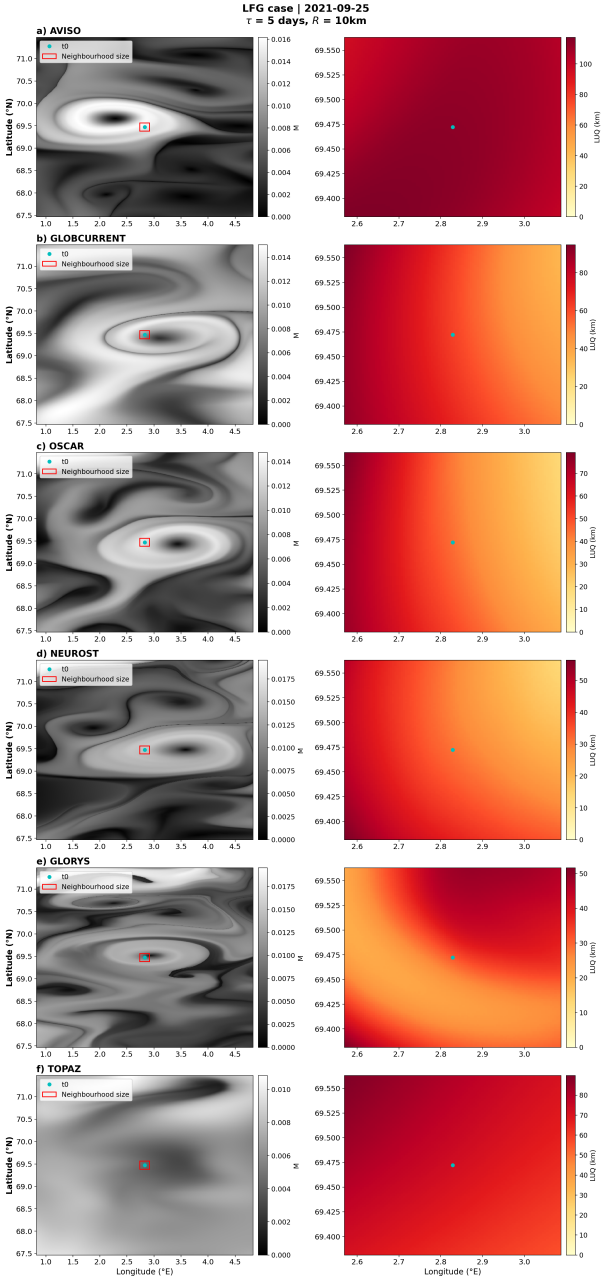

Figure 12. Lagrangian diagnostics for the Lofoten Gyre (LFG) case study on 25 September 2021, computed using an integration time scale of $\tau = 5$ days and a spatial neighbourhood of size $R = 10$ km (red square). Each row shows the results for one surface current product. Left panels show the Lagrangian descriptor M, where sharp gradients highlight the dynamical organization of the mesoscale recirculation and associated transport barriers. The cyan dot represents the observed drifter position, and the red box encloses the initial spatial neighbourhood. Right panels show the corresponding L_{UQ} fields, representing the geodesic distance between simulated particle positions and the observed terminal drifter position after $\tau = 5$ days.

https://doi.org/10.5194/egusphere-2026-3629
Preprint. Discussion started: 26 June 2026

are exported into a different transport corridor. From this perspective, differences between products are often better interpreted as shifts or distortions of the underlying transport structures than as stochastic perturbations of a common flow field. The comparison therefore, shows that products with a more realistic representation of mesoscale transport geometry perform better than products that only capture the broad current magnitude.

The Gulf Stream case provides a contrasting benchmark for an energetic boundary-current regime (Fig. 13). In this case, particle evolution is strongly controlled by the position, intensity, and lateral shear of the jet, together with the associated transport barriers identified by the Lagrangian descriptor. The corresponding L_{UQ} fields show that transport uncertainty is organized by the geometry of the boundary current and its frontal structures. Products that place the jet core and its associated transport barrier closer to those experienced by the observed drifter produce lower LUQ values, whereas products with a displaced or overly smoothed jet structure generate larger trajectory errors. This behaviour is particularly evident for products with coarser effective resolution or weaker representation of sharp frontal gradients.

Compared with the Lofoten Gyre, the Gulf Stream case shows that Lagrangian skill is not only limited by errors in recirculating structures, but also by the representation of narrow and energetic advective pathways. Products that better resolve the boundary-current structure maintain particles along the observed pathway for longer, whereas products that underestimate the jet intensity or misplace its position lead to rapid cross-stream or downstream separation. This comparison reinforces the idea that Lagrangian skill depends on the correct representation of transport geometry and its coherent structures, rather than on current speed alone.

Ocean circulation can be viewed as a collection of interacting time-dependent dynamical structures, including eddies, jets, recirculation regions, and transport barriers. At regional scales, these structures locally organize particle motion, while at basin scales they form a patchwork of interconnected transport systems. From this perspective, differences between ocean products and observations are often better interpreted as shifts, distortions, or changes in the underlying transport structures than as stochastic perturbations of a common flow field.

The Lagrangian diagnostics discussed above correspond to particular snapshots of the selected case studies and illustrate the dynamical mechanisms controlling transport uncertainty at specific dates. However, the relative performance of the different products may vary as the flow evolves and the observed drifter samples different transport regimes. To assess the temporal robustness of the Lagrangian validation, the LUQ analysis was repeated throughout the available observation period for each drifter case study.

Figures 14–16 summarize the resulting normalized LUQ diagnostics for the case studies grouped according to trajectory duration. The length of the analysis interval depends on the availability of drifter observations, leading to representative 30-, 60-, and 150-day case studies. This representation allows the comparison of product performance across trajectories with different spatial and temporal scales while preserving the dynamical contrast among regimes. Lower normalized LUQ values indicate that simulated particles remain closer to the observed drifter pathway, whereas higher values indicate larger accumulated transport deviations.

For the 30-day cases (Fig. 14), the Lofoten Gyre exhibits the largest normalized LUQ values, confirming that recirculating mesoscale regimes are particularly sensitive to small differences in the underlying transport geometry. In this regime, the

https://doi.org/10.5194/egusphere-2026-3629
Preprint. Discussion started: 26 June 2026

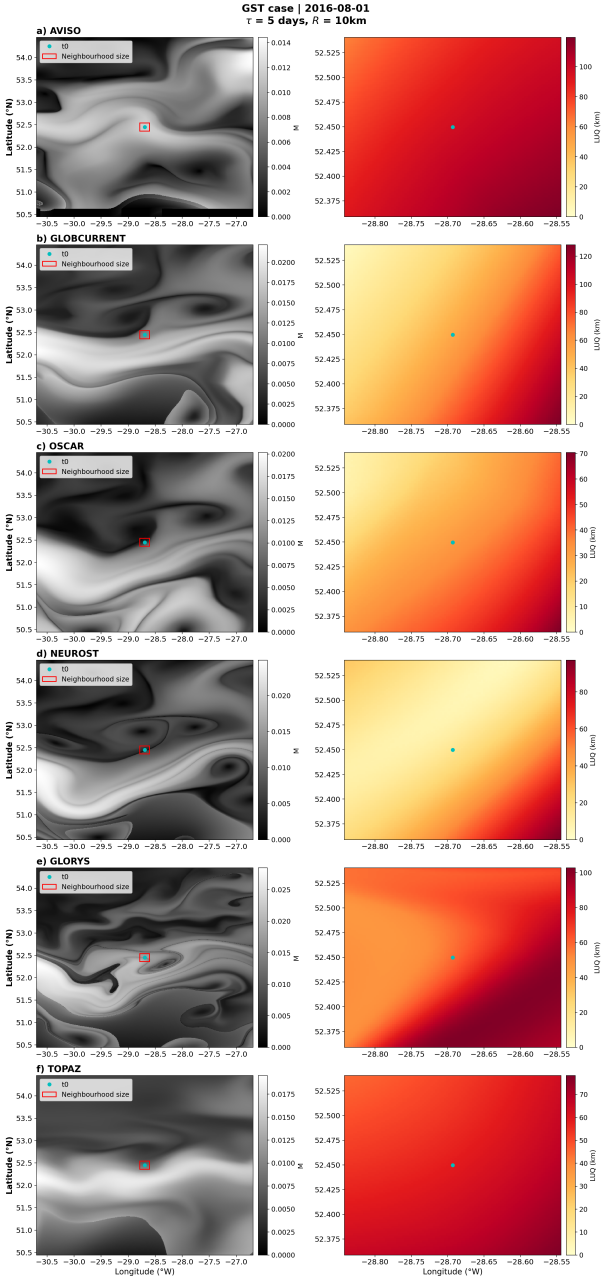

Figure 13. Lagrangian diagnostics for the Gulf Stream (GST) case study on 01 August 2016, computed using an integration time scale of $\tau = 5$ days and a spatial neighbourhood of size $R = 10$ km (red square). Each row shows the results for one surface current product. Left panels show the Lagrangian descriptor M, where sharp gradients identify the dynamical organization of the energetic boundary current and associated transport barriers. The cyan dot represents the observed drifter position, and the red box encloses the initial spatial neighbourhood. Right panels show the corresponding L_{UQ} fields, representing the geodesic distance between simulated particle positions and the observed terminal drifter position after $\tau = 5$ days.

https://doi.org/10.5194/egusphere-2026-3629
Preprint. Discussion started: 26 June 2026

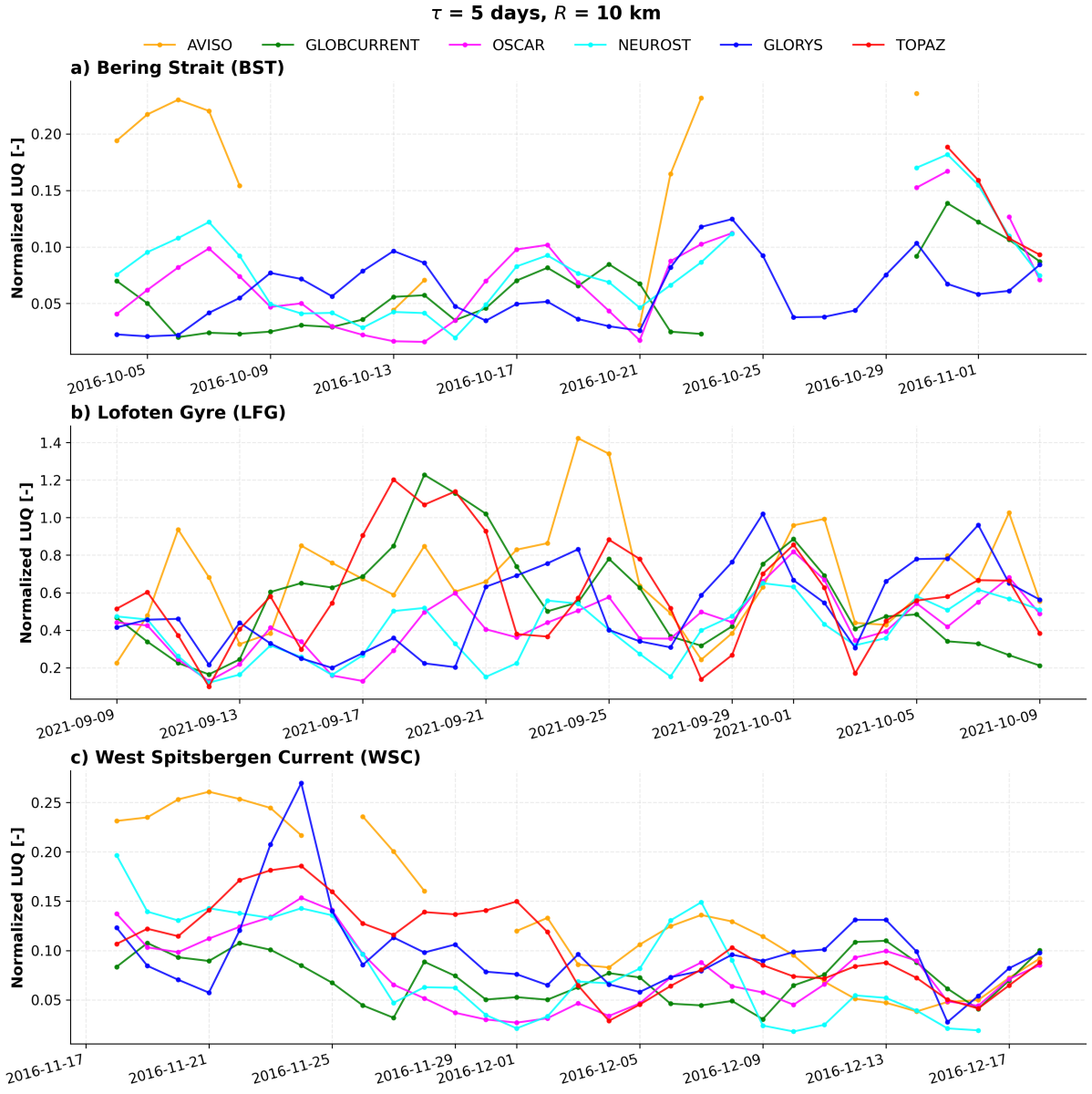

Figure 14. Temporal evolution of the normalized spatially averaged L_{UQ} values for the 30-day case studies: Bering Strait (BST), Lofoten Gyre (LFG), and West Spitsbergen Current (WSC). These values are normalized by the characteristic length of the corresponding drifter trajectory. Each panel corresponds to a case study, and the coloured curves represent the different surface current products. Lower normalized LUQ values indicate better Lagrangian agreement with the observed drifter trajectories. The Lofoten Gyre exhibits the largest normalized LUQ values, highlighting the difficulty of reproducing compact mesoscale recirculation, whereas the Bering Strait and West Spitsbergen Current generally show lower values for products that better capture gateway and boundary-current transport.

https://doi.org/10.5194/egusphere-2026-3629
Preprint. Discussion started: 26 June 2026

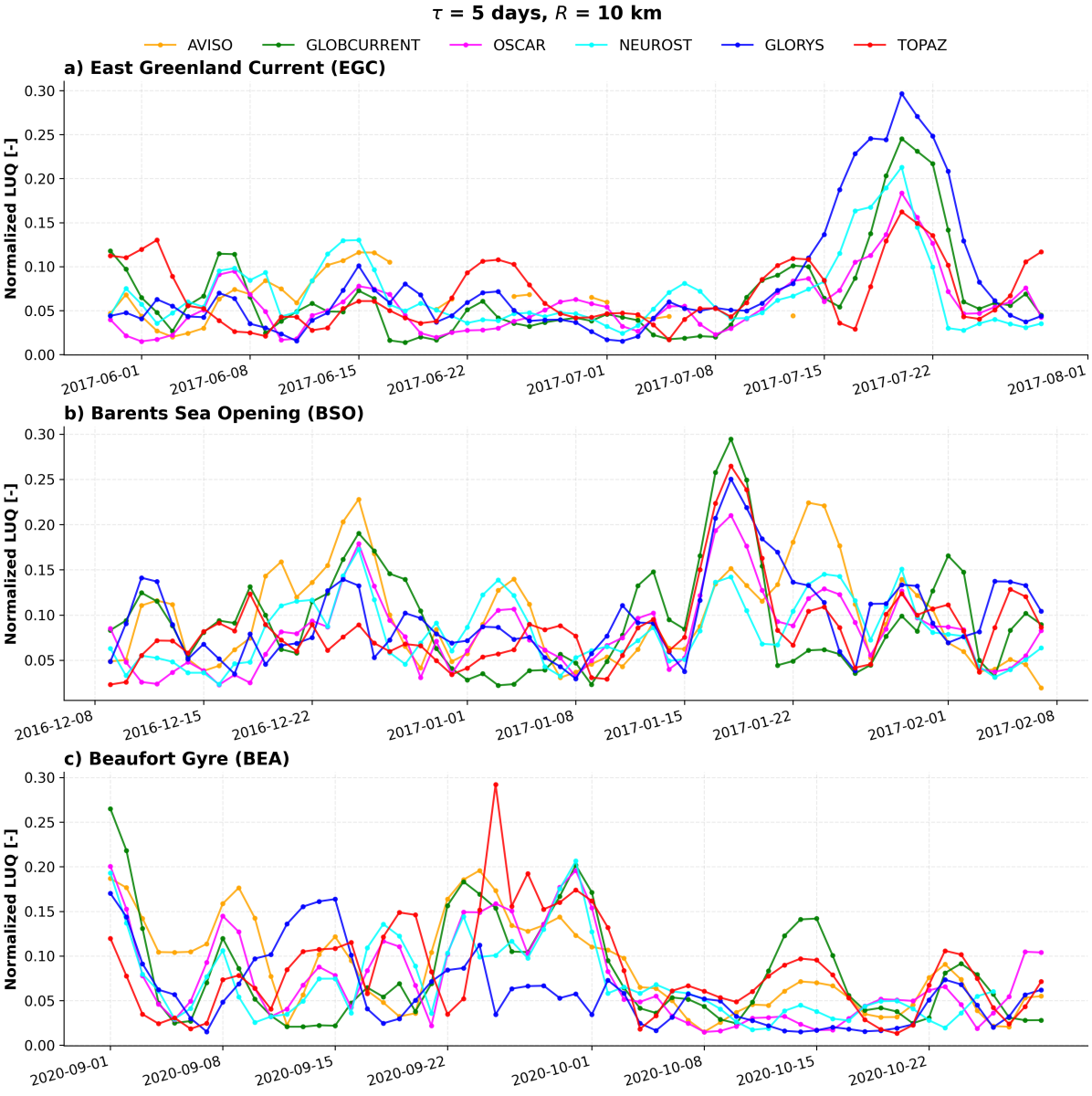

Figure 15. Temporal evolution of the normalized spatially averaged L_{UQ} values for the 60-day case studies: East Greenland Current (EGC), Barents Sea Opening (BSO), and Beaufort Gyre (BEA). These values are normalized by the characteristic length of the corresponding drifter trajectory. Each panel corresponds to a case study, and the coloured curves represent the different surface current products. Lower normalized LUQ values indicate better Lagrangian agreement with the observed drifter trajectories. The East Greenland Current and Barents Sea Opening generally exhibit lower LUQ values, reflecting the more coherent nature of along-slope and gateway transport, whereas the Beaufort Gyre shows larger inter-product variability associated with the influence of wind forcing, sea ice, and upper-ocean stratification.

https://doi.org/10.5194/egusphere-2026-3629
Preprint. Discussion started: 26 June 2026

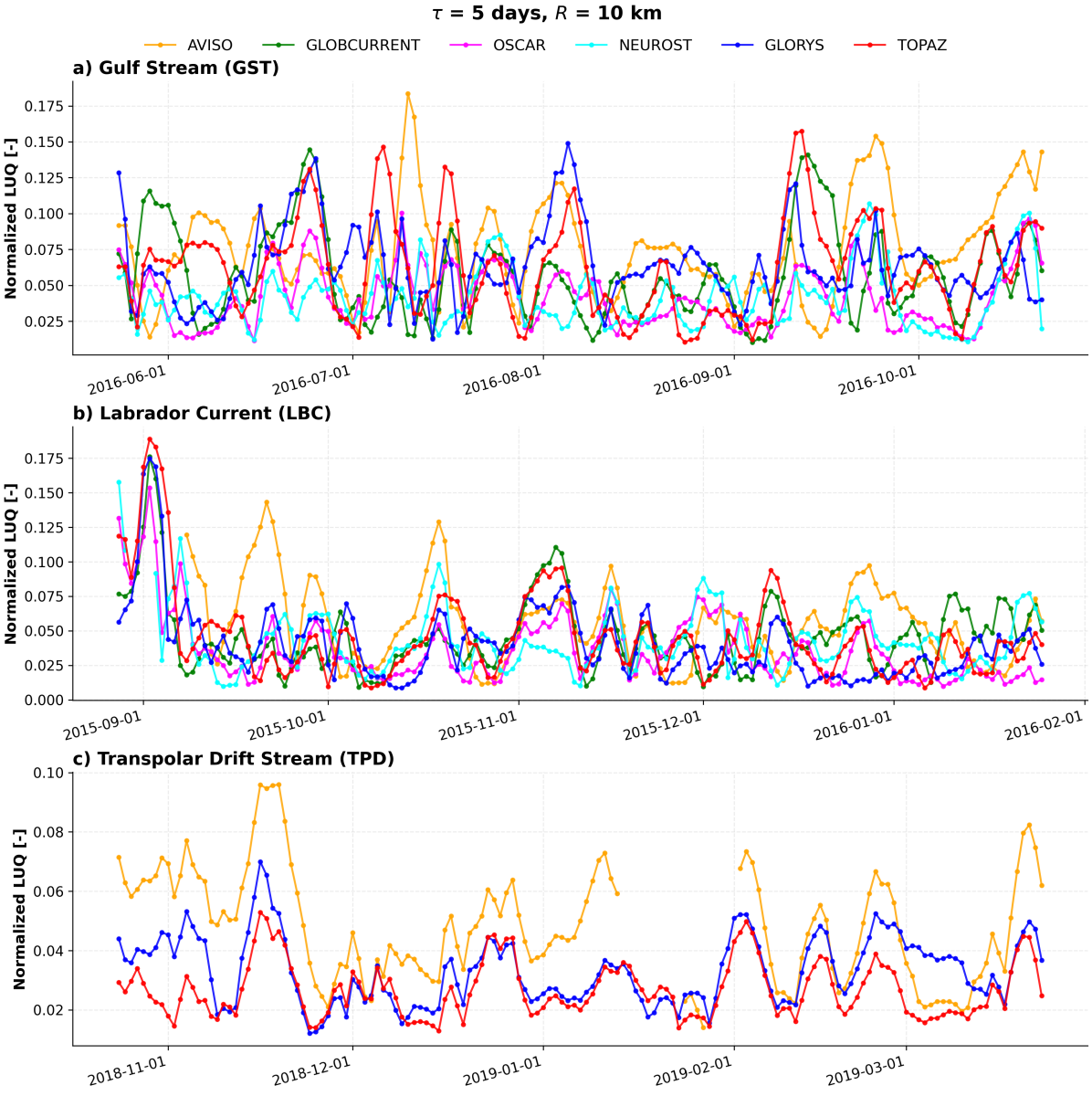

Figure 16. Temporal evolution of the normalized spatially averaged L_{UQ} values for the 150-day case studies: Gulf Stream (GST), Labrador Current (LBC), and Transpolar Drift (TPD). These values are normalized by the characteristic length of the corresponding drifter trajectory. Each panel corresponds to a case study, and the coloured curves represent the different surface current products. Lower normalized LUQ values indicate better Lagrangian agreement with the observed drifter trajectories. The Gulf Stream and Labrador Current generally show lower LUQ values for products that better reproduce boundary-current transport, whereas the Transpolar Drift exhibits larger inter-product variability associated with long-range Arctic transport influenced by sea ice, wind forcing, and sparse observational constraints.

https://doi.org/10.5194/egusphere-2026-3629
Preprint. Discussion started: 26 June 2026

best-performing products are those that more accurately reproduce the position of the gyre core and its associated transport barriers. By contrast, products that smooth or displace the gyre core show much larger LUQ values. The Bering Strait and West Spitsbergen Current cases show lower trajectory deviations for several products, especially those including near-surface or mixed-layer contributions, reflecting the more coherent and advective nature of gateway and boundary-current transport.

The 60-day cases (Fig. 15) show intermediate behaviour. The East Greenland Current and Barents Sea Opening are dominated by relatively coherent along-slope or gateway transport, and products that better capture topographic steering and boundary-current position show lower LUQ values. Reanalysis and multi-observational products generally perform better in these dynamically constrained regimes than products relying only on geostrophic balance. In the Beaufort Gyre, however, the spread among products is larger, reflecting the influence of wind forcing, sea-ice cover, and upper-ocean stratification. TOPAZ performs particularly well in this ice-influenced regime, suggesting that the inclusion of coupled ocean–sea-ice dynamics can improve the representation of transport pathways under sea-ice conditions.

The 150-day cases (Fig. 16) provide a longer-term test of transport consistency. Over these extended integrations, even small velocity differences can accumulate into substantial trajectory deviations. In the Gulf Stream and Labrador Current cases, the lowest LUQ values are obtained by products that better reproduce the position and intensity of the boundary current, while products with smoother or displaced current cores show larger accumulated errors. The Transpolar Drift case is especially demanding because it involves long-range Arctic transport influenced by sea ice, wind forcing, and sparse observational constraints. In this case, products with stronger Arctic-specific dynamical constraints, particularly TOPAZ and GLORYS, tend to provide more consistent pathways than products with limited coverage or purely geostrophic dynamics.

The LUQ diagnostics show that Lagrangian skill is strongly regime-dependent. Products that perform well in Eulerian velocity comparisons, such as NeurOST and OSCAR, generally tend to produce more realistic trajectories in several open-ocean and ice-free regimes, but the correspondence is not one-to-one. In ice-influenced or bathymetrically constrained regions, reanalysis products such as TOPAZ and GLORYS can perform comparatively better, even when their global Eulerian statistics are not the strongest. Conversely, AVISO tends to produce larger LUQ values in several cases, consistent with the limitations of using purely geostrophic currents to reproduce the full near-surface motion sampled by drifters.

More specifically, the case-study comparison further illustrates that products with with similar local velocity agreement can produce markedly different transport outcomes. This is particularly evident in regions where particle motion is controlled by narrow boundary currents, recirculating structures, or dynamically active transport barriers. Across gateway and boundary-current cases, normalized LUQ values are generally lower than in the Lofoten Gyre, suggesting that coherent advective pathways are more consistently reproduced than mesoscale retention regimes. Nevertheless, small shifts in the position of boundary currents or inflow pathways can lead to substantial downstream trajectory differences, especially in narrow passages such as the Bering Strait, the Barents Sea Opening, and the West Spitsbergen Current.

In the freshwater export and subpolar current cases, including the East Greenland Current and Labrador Current, product performance depends strongly on the representation of along-slope transport and topographic steering. Reanalysis and multi-observational products may better reproduce the dominant transport direction when the large-scale pathway is well constrained, whereas products relying mainly on geostrophic balance can be more sensitive to errors in the position and intensity of the

https://doi.org/10.5194/egusphere-2026-3629
Preprint. Discussion started: 26 June 2026

boundary current. In the Beaufort Gyre and Transpolar Drift, trajectory differences may arise not only from product limitations but also from intrinsic transport sensitivity, unresolved variability, wind forcing, sea-ice influence, and strong upper-ocean stratification.

Taken together, these results confirm that Eulerian and Lagrangian diagnostics evaluate complementary aspects of product performance. Eulerian metrics quantify local agreement with observed velocities, whereas the LUQ framework assesses how velocity differences accumulate into transport deviations while accounting for the dynamical structures that organize the flow. Their combined use therefore provides a more physically consistent assessment of Arctic surface current products for applications involving freshwater redistribution, tracer transport, and exchange pathways between the Arctic and the North Atlantic.

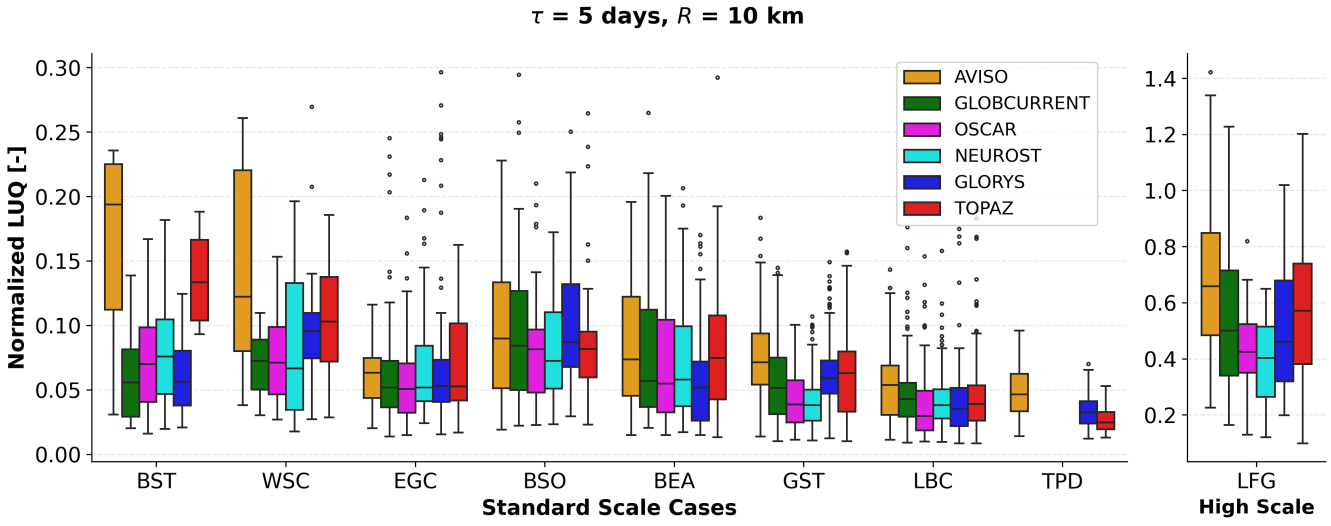

Figure 17. Case-study boxplots comparing the normalized LUQ performance of the evaluated surface current products. For each case study and product, the boxes and whiskers represent the temporal distribution of the normalized spatially averaged L_{UQ} values, computed at different dates t_0 over the duration of the corresponding drifter record. The case studies correspond to the drifter trajectories shown in Fig. 3: Bering Strait (BST), West Spitsbergen Current (WSC), East Greenland Current (EGC), Barents Sea Opening (BSO), Beaufort Gyre (BEA), Gulf Stream (GST), Labrador Current (LBC), and Transpolar Drift (TPD). The Lofoten Gyre (LFG) is shown separately in the right panel using an expanded y-axis because of its substantially larger normalized LUQ values. Product colours are AVISO (orange), GlobCurrent (green), OSCAR (magenta), NeurOST (cyan), GLORYS (blue), and TOPAZ (red).

The temporal evolution of the normalized spatially averaged L_{UQ} values for the different case studies shown in Figs. 14–16 is summarized in Figure 17. This figure presents the boxplots of the normalized spatially averaged L_{UQ} values for the selected case studies, providing a synthetic representation of their temporal variability across the different surface current products. The results reveal a strong dependence of Lagrangian skill on the dynamical regime and on the physical content of each product. Overall, the lowest LUQ values are generally obtained by products that include either mixed-layer dynamics, multiple

https://doi.org/10.5194/egusphere-2026-3629
Preprint. Discussion started: 26 June 2026

observational constraints, or model-based dynamical consistency, whereas purely geostrophic products show larger trajectory deviations in several regimes. OSCAR and GlobCurrent tend to perform well in advective boundary-current and gateway cases, consistent with their inclusion of wind-driven or near-surface current components. GLORYS and TOPAZ also show competitive performance in several dynamically constrained regions, with TOPAZ displaying particularly good behaviour in ice-influenced cases. In contrast, AVISO often exhibits larger LUQ values, reflecting the limitations of using a purely geostrophic altimetry-based product to reproduce the full near-surface motion sampled by drogued drifters.

The Lofoten Gyre stands out as the most challenging case, with substantially larger normalized LUQ values than the other regimes. This reflects the strong sensitivity of particle pathways to the precise location and structure of the mesoscale recirculation. In this case, the products differ markedly in their ability to place the recirculating structure sampled by the observed drifter. Products that more accurately capture the position of the gyre core and its associated transport barriers produce lower LUQ values, whereas products that displace or smooth the mesoscale circulation generate rapid trajectory divergence. This behavior explains why large transport deviations may arise even when local Eulerian velocity statistics are not necessarily the poorest. Additionally, the Lofoten Gyre is also the smallest-scale transport feature among the circulation regimes considered in this study, making it particularly difficult to resolve with coarse-resolution products. The challenge of accurately reproducing transport through small mesoscale structures has also been discussed by García-Sánchez et al. (2025).

Across the remaining cases, inter-product differences indicate that good Eulerian agreement does not always guarantee realistic Lagrangian behaviour. NeurOST and OSCAR, which show strong Eulerian skill in the global statistics, generally provide more realistic trajectories in several cases, but the correspondence is not one-to-one. Reanalysis products such as GLORYS and TOPAZ can outperform satellite-only products in regions where the transport pathway is strongly constrained by bathymetry, sea ice, or large-scale circulation. Conversely, products that reproduce local velocities reasonably well may still generate divergent trajectories if the underlying transport structures are displaced, overly smoothed, or dynamically incomplete.

5 Discussion

This study provides a combined Eulerian and Lagrangian assessment of six Arctic surface current products against drogued drifter observations. The results highlight that evaluating Arctic near-surface circulation requires more than point-wise velocity comparisons. Although Eulerian diagnostics identify products that reproduce local current speed and direction more accurately, they do not necessarily assess whether the underlying flow structures responsible for organizing transport are realistically represented. The Lagrangian analysis shows that small differences in the velocity field, as well as shifts or distortions in the associated transport structures, can accumulate into substantial deviations in transport pathways, retention, and connectivity. From this perspective, realistic transport depends not only on local velocity agreement but also on the correct representation of the transport geometry governing particle motion. This distinction is particularly important in the Arctic Ocean, where freshwater redistribution and exchanges with the North Atlantic depend on cumulative transport processes rather than on instantaneous velocity agreement alone.

https://doi.org/10.5194/egusphere-2026-3629
Preprint. Discussion started: 26 June 2026

5.1 Product performance and the role of represented dynamics

The Eulerian results show that product performance depends strongly on the dynamical content of each dataset. NeurOST and OSCAR provide the best overall agreement with drifter-derived velocities, but for different reasons. NeurOST improves the representation of geostrophic surface circulation through a machine-learning reconstruction of sea surface height constrained by nadir altimetry and high-resolution sea surface temperature, whereas OSCAR explicitly includes wind-driven and mixed-layer contributions. Their improved performance relative to conventional altimetry-only geostrophic currents indicates that additional observational constraints or near-surface dynamical information are important for reproducing the motion sampled by drogued drifters.

GlobCurrent and GLORYS show intermediate skill. GlobCurrent reproduces the mean observed current speed particularly well, consistent with the use of total currents at a depth comparable to the nominal drogue depth of the GDP drifters. However, its smoother distribution suggests that part of the observed small-scale variability is reduced by the combination of geostrophic and Ekman components. GLORYS captures part of the large-scale circulation variability through dynamically consistent model physics and data assimilation, but, as with other gridded products, finite resolution and assimilation procedures may smooth near-surface velocity extremes and sharp transport structures.

AVISO and TOPAZ show weaker agreement in the global speed-based Eulerian statistics. For AVISO, this is consistent with its purely geostrophic formulation, which does not explicitly include wind-driven, inertial, or other ageostrophic contributions sampled by the drifters. TOPAZ, despite being a regional ocean–sea-ice reanalysis optimized for high latitudes, shows weaker near-surface speed agreement than the best-performing products in the global statistics. This suggests that a dynamically consistent ocean–ice model framework does not necessarily guarantee improved agreement with drogued drifter velocities, particularly when near-surface currents, narrow gateways, or small-scale transport barriers are involved.

5.2 Regional and seasonal dependence of current-product skill

The Eulerian analysis also reveals strong seasonal and regional variability in product skill. Most products perform better during summer and worse during winter and early spring, reflecting the combined influence of sea-ice cover, satellite sampling, wind-driven variability, and the uneven seasonal distribution of drifter observations. These seasonal differences are important because Arctic freshwater storage and export are strongly modulated by seasonal changes in sea ice, stratification, and atmospheric forcing.

Regionally, the largest errors occur in dynamically complex areas, including shallow shelves, narrow Arctic gateways, Pacific and Atlantic inflow pathways, and boundary-current systems. These regions are characterized by strong bathymetric steering, mesoscale variability, ice-ocean interactions, and sharp velocity gradients. In such regimes, small spatial displacements of a current core or recirculating structure can generate large point-wise velocity errors even when the broad circulation pattern is qualitatively represented. The spatial error maps therefore demonstrate that product skill cannot be interpreted as a single Arctic-wide property, but must be evaluated in relation to the circulation regime and intended application.

https://doi.org/10.5194/egusphere-2026-3629
Preprint. Discussion started: 26 June 2026

The generally weaker performance of altimetry-only geostrophic currents in these regions highlights the importance of ageostrophic and mixed-layer dynamics for Arctic near-surface transport. Wind forcing, Ekman currents, inertial variability, and sea-ice interactions can contribute substantially to the motion of drogued drifters, especially over shelves, marginal ice zones, and gateways. Products that include some of these contributions tend to perform better, although no product performs uniformly best across all seasons and regions.

5.3 Good Eulerian skill does not necessarily imply realistic transport pathways

A central result of this study is that good Eulerian agreement does not necessarily imply realistic Lagrangian transport pathways. The LUQ diagnostics show that transport deviations depend not only on local velocity differences, but also on the representation of the transport geometry organizing particle motion. The position of boundary currents, recirculating gyres, and transport barriers can determine whether particles remain trapped, follow the observed pathway, or are diverted into alternative transport corridors.

This behavior is clearly illustrated by the Lofoten Gyre case. The Lagrangian descriptor analysis shows that differences between products are not only related to current magnitude, but also to the representation of the mesoscale recirculation and its associated transport topology. A relatively small displacement of the vortex core can place the observed drifter near the edge of a retention region rather than inside it, producing large LUQ values after only a few days of integration. This explains why recirculating and mesoscale-dominated regimes exhibit larger normalized LUQ values than more advective gateway or boundary-current cases.

The LUQ-based metrics further show that Lagrangian skill is strongly regime-dependent. Shorter 30-day cases already reveal large differences between advective and recirculating regimes, while the 60-day and 150-day cases demonstrate how small velocity differences can accumulate over longer time scales. In recirculating regimes, transport is particularly sensitive to the correct representation of retention structures and their associated transport barriers. By contrast, in energetic boundary-current systems such as the East Greenland Current, Labrador Current, and Gulf Stream, product performance depends strongly on the correct positioning and intensity of along-slope flow. Even modest differences in these features can produce substantial downstream transport deviations as particles are advected over long distances. In Arctic pathways such as the Beaufort Gyre and Transpolar Drift, trajectory differences are additionally affected by wind forcing, sea-ice influence, and strong sensitivity to initial conditions.

5.4 Added value of uncertainty-aware Lagrangian diagnostics

The LUQ framework provides an uncertainty-aware interpretation of trajectory agreement. Direct trajectory-to-trajectory comparisons may be overly restrictive because neighbouring trajectories do not evolve independently, but are organized by the coherent transport structures of the underlying flow. By evaluating transport consistency over a spatial neighbourhood around the observed drifter position, LUQ helps distinguish between systematic product errors and trajectory differences associated with intrinsic transport variability.

https://doi.org/10.5194/egusphere-2026-3629
Preprint. Discussion started: 26 June 2026

This is particularly relevant for Arctic applications, where drifter observations are sparse and transport pathways are often controlled by evolving mesoscale structures, ice-ocean interactions, and flow barriers. The LUQ diagnostics show that deviations between simulated and observed trajectories should not always be interpreted as product deficiencies alone. Instead, part of these deviations reflects the intrinsic transport geometry of the flow, where neighbouring particles may experience markedly different dynamical evolutions because they lie on opposite sides of coherent transport structures or within distinct transport regimes. By explicitly accounting for this spatial organization of transport deviations, the LUQ framework interprets uncertainty as a property of the transport geometry rather than solely as a measure of trajectory separation. As a result, uncertainty-aware Lagrangian diagnostics provide a more physically meaningful assessment of transport consistency than direct trajectory-to-trajectory separation metrics.

For studies of freshwater redistribution, tracer transport, and connectivity between Arctic gateways, this distinction is crucial. A product that performs well in Eulerian metrics may still misrepresent transport pathways if it displaces a boundary current or recirculation feature. Conversely, a product with moderate local velocity agreement may still capture the dominant pathway if the large-scale transport geometry is well represented. Combining Eulerian and LUQ-based diagnostics therefore provides a more complete assessment of product suitability for transport applications.

The LUQ analysis further suggests that no single surface current product provides the most realistic representation of transport across all Arctic dynamical regimes. Products incorporating different physical processes or observational constraints may better reproduce particular transport structures, such as energetic boundary currents, recirculating gyres, or ice-influenced pathways. The suitability of a given product therefore depends not only on its overall statistical performance, but also on the transport processes and spatial scales relevant to the intended application.

5.5 Limitations and implications for future Arctic current validation

Several limitations should be considered when interpreting the results. First, drifter observations are unevenly distributed in space and time, with limited coverage in persistently ice-covered regions. As a result, the validation primarily reflects seasonally ice-free and marginal-ice-zone conditions rather than the full central Arctic Ocean. Second, the evaluated products do not represent identical physical quantities or effective depths. AVISO and NeurOST provide geostrophic currents, GlobCurrent and OSCAR include total or mixed-layer near-surface contributions, and GLORYS and TOPAZ are model-based reanalyses. The comparison with drogued drifters should therefore be interpreted as an assessment of near-surface transport realism, not as a strict comparison of equivalent dynamical quantities.

Third, the Lagrangian analysis depends on methodological choices, including the integration time scale, spatial neighbourhood size, and trajectory duration. The selected configuration of $\tau = 5$ days and $R = 10$ km is a compromise. The integration time τ should be sufficiently long for transport differences to emerge, while remaining consistent with the characteristic time scales of the transport process under investigation. The neighbourhood size R should be large enough to capture the influence of nearby transport structures, but not so large that it spans a substantial fraction of the trajectory travelled over the integration interval. Finally, the case studies provide a targeted evaluation of representative transport pathways, but they do not exhaust the full range of Arctic circulation variability.

https://doi.org/10.5194/egusphere-2026-3629
Preprint. Discussion started: 26 June 2026

Despite these limitations, the combined Eulerian–Lagrangian framework developed here provides a robust approach for evaluating Arctic surface current products. The results emphasize that no single product is uniformly optimal across all Arctic circulation regimes and applications. Instead, different products may better represent different physical processes and transport regimes, so product selection should be guided by the intended application and the dominant transport scales involved. For studies focused on local velocity variability, Eulerian skill may be the most relevant criterion. For studies of freshwater pathways, tracer transport, and connectivity, Lagrangian diagnostics are essential because they evaluate the cumulative impact of velocity-field differences on transport pathways and the underlying transport geometry. Improving Arctic surface current products will require not only better local velocity estimates, but also a more realistic representation of the transport geometry that governs Arctic connectivity across multiple spatial and temporal scales.

6 Conclusions

This study provides a combined Eulerian and Lagrangian evaluation of six Arctic surface current products using drogued drifter observations from the Global Drifter Program over the 2011–2021 period. The evaluated products include altimetry-derived geostrophic currents, machine-learning reconstructions of geostrophic currents, total or mixed-layer surface current products, and ocean reanalyses. Because these datasets represent different dynamical components and effective depths, the comparison was interpreted as an assessment of their ability to reproduce the near-surface motion sampled by drifters rather than as a strict comparison of identical physical quantities.

The Eulerian analysis shows that product skill varies strongly by season and region. NeurOST and OSCAR provide the best overall agreement with drifter-derived velocities, while GlobCurrent and GLORYS show intermediate performance, TOPAZ exhibits weaker near-surface speed agreement, and AVISO tends to underestimate current intensity and variability. These results indicate that products incorporating additional observational constraints, wind-driven contributions, or mixed-layer dynamics generally better reproduce the near-surface circulation sampled by drifters than conventional altimetry-only geostrophic currents.

Regional differences are substantial. The largest errors occur in dynamically complex areas such as Arctic gateways, shallow shelves, boundary-current systems, and regions affected by sea-ice interactions and strong mesoscale variability. These results show that product performance cannot be described by a single Arctic-wide metric, but depends on the circulation regime, season, and intended application.

The Lagrangian analysis demonstrates that good local velocity agreement does not necessarily translate into realistic transport pathways. Small velocity differences, as well as shifts in the transport structures organizing the flow, can accumulate during trajectory integration and produce large deviations in particle pathways, retention, and connectivity. This is particularly evident in recirculating and mesoscale-dominated regimes such as the Lofoten Gyre, where small displacements of the vortex core or associated transport barriers can strongly affect the simulated pathway.

The LUQ framework provides an uncertainty-aware assessment of trajectory agreement by accounting for the dynamical organization of transport deviations. Rather than treating trajectory differences as random perturbations, LUQ relates them to the

https://doi.org/10.5194/egusphere-2026-3629
Preprint. Discussion started: 26 June 2026

coherent transport structures governing particle motion. This is especially valuable in the Arctic Ocean, where observations are sparse and transport pathways are strongly influenced by mesoscale structures, sea ice, wind forcing, and bathymetric steering. The LUQ results show that part of the apparent mismatch between observed and simulated trajectories is due to differences in the underlying transport geometry and the associated sensitivity of transport pathways to nearby initial conditions, rather than systematic product errors alone.

Overall, our results demonstrate that Eulerian and Lagrangian diagnostics provide complementary information for the evaluation of Arctic surface current products. Eulerian metrics are essential for assessing local velocity agreement, whereas Lagrangian diagnostics evaluate the cumulative impact of velocity-field errors on transport pathways while accounting for the transport structures organizing the flow. Combining both approaches provides a physically consistent framework for evaluating Arctic surface current products and for selecting the most appropriate dataset according to the circulation regime, the transport processes, and spatial and temporal scales relevant to a given application.

Code availability. The Eulerian and Lagrangian implementations are provided as modular Python packages and are publicly available in the Barcelona Polar Lab GitHub repository (FRESH-CARE, Work Package 1): https://github.com/Barcelona-Polar-Lab/FRESH-CARE/tree/main/WP1/Ocean_currents. The exact software and code used to reproduce this research are archived and citable on Zenodo: https://doi.org/10.5281/zenodo.20624431.

Data availability. The observational and reanalysis datasets used in this study are publicly accessible through their respective public repositories, with further descriptions provided in the Data section. Specifically, global ocean satellite observations from AVISO are available through the Copernicus Marine Service (CMEMS) platform at https://doi.org/10.24400/527896/a01-2020.001 (Lellouche et al., 2021), while GLOBCURRENT configuration and surface current fields are accessible via CMEMS at https://doi.org/10.48670/mds-00327 (Rio et al., 2014). Surface current data from OSCAR and altimetry information from NEUROST are archived at https://doi.org/10.5067/OSCAR-25F20 (Dohan, 2021) and https://doi.org/10.5067/NEURO-STV24 (OSTST, 2024), respectively. Regarding reanalysis products, daily surface current velocities from the GLORYS GLOBAL_MULTIYEAR_PHY_001_030 product are distributed through CMEMS at https://doi.org/10.48670/moi-00021, and daily Arctic surface current velocities from the TOPAZ ARCTIC_MULTIYEAR_PHY_002_003 product are available at https://doi.org/10.48670/moi-00007. Finally, the Global Drifter Program dataset is hosted by the NOAA National Centers for Environmental Information (NCEI) and can be accessed at https://doi.org/10.25921/7ntx-z961.

Author contributions. A.R-E. and M.U. conceptualized the study. A.R-E., J.C., L.Y., A.M., and M.U. developed the methodology. A.R-E., J.C., L.Y., and A.M. contributed to software development. Validation was performed by A.R-E., J.C., A.M., and M.U. Formal analysis was carried out by A.R-E., J.C., and M.U. A.R-E., J.C., A.M., and M.U. conducted the investigation. Data curation was managed by J.C. and A.R-E., who also handled data visualization. A.R-E. and M.U. prepared the original draft, while A.R-E., J.C., L.Y., A.M., and M.U. participated in writing, review, and editing. A.M. and M.U. provided supervision, project administration, and funding acquisition.

https://doi.org/10.5194/egusphere-2026-3629
Preprint. Discussion started: 26 June 2026

Competing interests. The authors declare no competing interests.

Acknowledgements. This research has received funding from the European Research Council (ERC) under the European Union's Horizon Europe research and innovation programme, Grant Agreement No. 10116451 (FRESH-CARE). A.R-E. was supported by a fellowship from the CSIC JAE Intro ICU 2025 call, funded by the Spanish Ministry of Science, Innovation and Universities (Grant Ref: PolarCSIC-01). AMM acknowledges the support from grant PID2021-123348OB-I00 funded by MCIN/AEI/10.13039/501100011033/ and by FEDER A way to make Europe.

We also acknowledge funding from the Spanish government through the 'Severo Ochoa Centre of Excellence' accreditation (Grant CEX2024-001494-S funded by AEI 10.13039/501100011033). This work is a contribution to CSIC Conexión Polar and CSIC Thematic Interdisciplinary Platform PTI Teledetect.

https://doi.org/10.5194/egusphere-2026-3629
Preprint. Discussion started: 26 June 2026

References

Armitage, T. W. K., Bacon, S., Ridout, A. L., Thomas, S. F., Aksenov, Y., and Wingham, D. J.: Arctic sea surface height variability and change from satellite radar altimetry and GRACE, 2003–2014, Journal of Geophysical Research: Oceans, 121, 4303–4322, https://doi.org/10.1002/2015JC011579, 2016.

Armitage, T. W. K., Bacon, S., Ridout, A. L., Petty, A. A., Wolbach, S., and Tsamados, M.: Arctic Ocean surface geostrophic circulation 2003–2014, The Cryosphere, 11, 1767–1780, https://doi.org/10.5194/tc-11-1767-2017, 2017.

Barron, C., Smedstad, L., Dastugue, J., and Smedstad, O.: Evaluation of ocean models using observed and simulated drifter trajectories: Impact of sea surface height on synthetic profiles for data assimilation, J. Geophys. Res.: Ocean, 112, https://doi.org/10.1029/2006JC003982, 2007.

Bleck, R.: An oceanic general circulation model framed in hybrid isopycnic-Cartesian coordinates, Ocean Modelling, 4, 55–88, https://doi.org/10.1016/S1463-5003(01)00012-9, 2002.

Bonjean, F. and Lagerloef, G. S. E.: Diagnostic Model and Analysis of the Surface Currents in the Tropical Pacific Ocean, Journal of Physical Oceanography, 32, 2938–2954, https://doi.org/10.1175/1520-0485(2002)032<2938:DMAAOT>2.0.CO;2, 2002.

Chiswell, S. M. and Rickard, G. J.: Eulerian and Lagrangian statistics in the Bluelink numerical model and AVISO altimetry: Validation of model eddy kinetics, Journal of Geophysical Research: Oceans, 113, 2007JC004 673, https://doi.org/10.1029/2007JC004673, 2008.

Dohan, K.: Ocean surface currents from satellite data, Journal of Geophysical Research: Oceans, 122, 2647–2651, https://doi.org/10.1002/2017JC012961, 2017.

Dohan, K.: Ocean Surface Current Analyses Real-time (OSCAR) Surface Currents - Final 0.25 Degree, https://doi.org/10.5067/OSCAR-25F20, 2021.

Drange, H. and Simonsen, K.: Formulation of air-sea fluxes in the ESOP2 version of MICOM, 125, Nansen Environmental and Remote Sensing Center Tech. Rep., 1996.

Fu, L.-L.: Determining Ocean Circulation and Sea Level from Satellite Altimetry: Progress and Challenges, p. 147–163, Springer Netherlands, Dordrecht, ISBN 9789048186808, https://doi.org/10.1007/978-90-481-8681-5_9, 2010.

García-Garrido, V. J., Mancho, A. M., Wiggins, S., and Mendoza, C.: A dynamical systems approach to the surface search for debris associated with the disappearance of flight MH370, Nonlinear Processes in Geophysics, 22, https://doi.org/doi.org/10.5194/npg-22-701-2015, 2015.

García-Sánchez, G., Mancho, A. M., Ramos, A. G., Coca, J., Pérez-Gómez, B., álvarez Fanjul, E., Sotillo, M. G., García-León, M., García-Garrido, V. J., and Wiggins, S.: Very High Resolution Tools for the Monitoring and Assessment of Environmental Hazards in Coastal Areas, Frontiers in Marine Science, 7, https://doi.org/10.3389/fmars.2020.605804, 2021.

García-Sánchez, G., Mancho, A. M., Ramos, A. G., Coca, J., and Wiggins, S.: Structured pathways in the turbulence organizing recent oil spill events in the Eastern Mediterranean, Scientific Reports, 12, https://doi.org/10.1038/s41598-022-07350-w, 2022a.

García-Sánchez, G., Mancho, A. M., and Wiggins, S.: A bridge between invariant dynamical structures and uncertainty quantification., Commun. Nonlinear Sci. Numer. Simul., 104, https://doi.org/10.1016/j.cnsns.2021.106016, 2022b.

García-Sánchez, G., Mancho, A. M., Agaoglou, M., and Wiggins, S.: New links between invariant dynamical structures and uncertainty quantification, Physica D, 453, https://doi.org/10.1016/j.physd.2023.133826, 2023.

García-Sánchez, G., Agaoglou, M., Smith, E. M. C., and Mancho, A. M.: A Lagrangian uncertainty quantification approach to validate ocean model datasets, Physica D: Nonlinear Phenomena, 476, 134 690, https://doi.org/10.1016/j.physd.2025.134690, 2025.

https://doi.org/10.5194/egusphere-2026-3629
Preprint. Discussion started: 26 June 2026

Haine, T. W., Curry, B., Gerdes, R., Hansen, E., Karcher, M., Lee, C., Rudels, B., Spreen, G., de Steur, L., Stewart, K. D., and Woodgate, R.: Arctic freshwater export: Status, mechanisms, and prospects, Global and Planetary Change, 125, 13–35, https://doi.org/10.1016/j.gloplacha.2014.11.013, 2015.

Hunke, E. C. and Dukowicz, J. K.: An Elastic–Viscous–Plastic Model for Sea Ice Dynamics, Journal of Physical Oceanography, 27, 1849–1867, https://doi.org/10.1175/1520-0485(1997)027%3C1849:AEVPMF%3E2.0.CO;2, 1997.

Lagerloef, G. S. E., Mitchum, G. T., Lukas, R. B., and Niiler, P. P.: Tropical Pacific near-surface currents estimated from altimeter, wind, and drifter data, Journal of Geophysical Research: Oceans, 104, 23 313–23 326, https://doi.org/10.1029/1999JC900197, 1999.

Lellouche, J.-M., Greiner, E., Bourdallé-Badie, R., Garric, G., Melet, A., Drévillon, M., Bricaud, C., Hamon, M., Le Galloudec, O., Regnier, C., Candela, T., Testut, C.-E., Gasparin, F., Ruggiero, G., Benkiran, M., Drillet, Y., and Le Traon, P.-Y.: The Copernicus Global 1/12° Oceanic and Sea Ice GLORYS12 Reanalysis, Frontiers in Earth Science, 9, https://doi.org/10.3389/feart.2021.698876, 2021.

Liu, Y. and Weisberg, R.: Evaluation of trajectory modeling in different dynamic regions using normalized cumulative Lagrangian separation, J. Geophys. Res.: Ocean., 116, https://doi.org/10.1029/2010JC006837, 2011.

Lumpkin, R. and Centurioni, L.: NOAA Global Drifter Program quality-controlled 6-hour interpolated data from ocean surface drifting buoys, https://doi.org/10.25921/7NTX-Z961, 2010.

Lumpkin, R. and Centurioni, L.: Global Drifter Program quality-controlled 6-hour interpolated data from ocean surface drifting buoys, https://doi.org/10.25921/7ntx-z961, 2019.

Lumpkin, R. and Pazos, M.: Measuring Surface Currents with Surface Velocity Program Drifters: The Global Drifter Program, Lagrangian Analysis and Prediction of Coastal and Ocean Dynamics, pp. 39–67, https://doi.org/10.1017/CBO9780511535901.003, 2007.

Lumpkin, R., Grodsky, S. A., Centurioni, L., Rio, M.-H., Carton, J. A., and Lee, D.: Removing Spurious Low-Frequency Variability in Drifter Velocities, Journal of Atmospheric and Oceanic Technology, 30, 353–360, https://doi.org/10.1175/JTECH-D-12-00139.1, 2013.

Mancho, A. M., Wiggins, S., Curbelo, J., and Mendoza, C.: Lagrangian Descriptors: A Method for Revealing Phase Space Structures of General Time Dependent Dynamical Systems, Communications in Nonlinear Science and Numerical Simulation, 18, https://doi.org/10.1016/j.cnsns.2013.05.002, 2013.

Martin, S. A., Manucharyan, G. E., and Klein, P.: Deep Learning Improves Global Satellite Observations of Ocean Eddy Dynamics, Geophysical Research Letters, 51, e2024GL110 059, https://doi.org/10.1029/2024GL110059, 2024.

Mendoza, C., Mancho, A. M., and Wiggins, S.: Lagrangian Descriptors and the Assessment of the Predictive Capacity of Oceanic Data Sets, Nonlinear Processes in Geophysics, 21, https://doi.org/10.5194/npg-21-677-2014, 2014.

OSTST: Daily NeurOST L4 Sea Surface Height and Surface Geostrophic Currents, https://doi.org/10.5067/NEURO-STV24, 2024.

Prandi, P., Poisson, J.-C., Faugère, Y., Guillot, A., and Dibarboure, G.: Arctic sea surface height maps from multi-altimeter combination, Earth System Science Data, 13, 5469–5482, https://doi.org/10.5194/essd-13-5469-2021, 2021.

Proshutinsky, A., Krishfield, R., Timmermans, M., Toole, J., Carmack, E., McLaughlin, F., Williams, W. J., Zimmermann, S., Itoh, M., and Shimada, K.: Beaufort Gyre freshwater reservoir: State and variability from observations, Journal of Geophysical Research: Oceans, 114, 2008JC005 104, https://doi.org/10.1029/2008JC005104, 2009.

Proshutinsky, A., Krishfield, R., Toole, J. M., Timmermans, M., Williams, W., Zimmermann, S., Yamamoto-Kawai, M., Armitage, T. W. K., Dukhovskoy, D., Golubeva, E., Manucharyan, G. E., Platov, G., Watanabe, E., Kikuchi, T., Nishino, S., Itoh, M., Kang, S., Cho, K., Tateyama, K., and Zhao, J.: Analysis of the Beaufort Gyre Freshwater Content in 2003–2018, Journal of Geophysical Research: Oceans, 124, 9658–9689, https://doi.org/10.1029/2019JC015281, 2019.

https://doi.org/10.5194/egusphere-2026-3629
Preprint. Discussion started: 26 June 2026

Pujol, M.-I., Faugère, Y., Taburet, G., Dupuy, S., Pelloquin, C., Ablain, M., and Picot, N.: DUACS DT2014: the new multi-mission altimeter data set reprocessed over 20 years, Ocean Science, 12, 1067–1090, https://doi.org/10.5194/os-12-1067-2016, 2016.

Rahmstorf, S., Box, J. E., Feulner, G., Mann, M. E., Robinson, A., Rutherford, S., and Schaffernicht, E. J.: Exceptional twentieth-century slowdown in Atlantic Ocean overturning circulation, Nature Climate Change, 5, 475–480, https://doi.org/10.1038/nclimate2554, 2015.

Reynolds, R. W., Smith, T. M., Liu, C., Chelton, D. B., Casey, K. S., and Schlax, M. G.: Daily High-Resolution-Blended Analyses for Sea Surface Temperature, Journal of Climate, 20, 5473–5496, https://doi.org/10.1175/2007JCLI1824.1, 2007.

Rio, M., Mulet, S., and Picot, N.: Beyond GOCE for the ocean circulation estimate: Synergetic use of altimetry, gravimetry, and in situ data provides new insight into geostrophic and Ekman currents, Geophysical Research Letters, 41, 8918–8925, https://doi.org/10.1002/2014GL061773, 2014.

Sakov, P. and Oke, P. R.: A deterministic formulation of the ensemble Kalman filter: an alternative to ensemble square root filters, Tellus A: Dynamic Meteorology and Oceanography, 60, 361, https://doi.org/10.1111/j.1600-0870.2007.00299.x, 2008.

Sakov, P., Counillon, F., Bertino, L., Lisæter, K. A., Oke, P. R., and Korablev, A.: TOPAZ4: an ocean-sea ice data assimilation system for the North Atlantic and Arctic, Ocean Science, 8, 633–656, https://doi.org/10.5194/os-8-633-2012, 2012.

Serreze, M. C. and Francis, J. A.: The Arctic Amplification Debate, Climatic Change, 76, 241–264, https://doi.org/10.1007/s10584-005-9017-y, 2006.

Shadden, S. C., Lekien, F., Paduan, J. D., Chavez, F. P., and Marsden, J. E.: The correlation between surface drifters and coherent structures based on high-frequency radar data in Monterey Bay, Deep Sea Research Part II: Topical Studies in Oceanography, 56, 161–172, https://doi.org/https://doi.org/10.1016/j.dsr2.2008.08.008, aOSN II: The Science and Technology of an Autonomous Ocean Sampling Network, 2009.

Sudre, F., Hernández-Carrasco, I., Mazoyer, C., Sudre, J., Dewitte, B., Garçon, V., and Rossi, V.: An ocean front dataset for the Mediterranean sea and southwest Indian ocean, Scientific Data, 10, 730, https://doi.org/10.1038/s41597-023-02615-z, 2023.

Traon, P. Y. L. and Dibarboure, G.: Velocity Mapping Capabilities of Present and Future Altimeter Missions: The Role of High-Frequency Signals, Journal of Atmospheric and Oceanic Technology, 19, 2077–2087, https://doi.org/10.1175/1520-0426(2002)019%3C2077:VMCOPA%3E2.0.CO;2, 2002.

Van Sebille, E., Griffies, S. M., Abernathey, R., Adams, T. P., Berloff, P., Biastoch, A., Blanke, B., Chassignet, E. P., Cheng, Y., Cotter, C. J., Deleersnijder, E., Döös, K., Drake, H. F., Drijfhout, S., Gary, S. F., Heemink, A. W., Kjellsson, J., Koszalka, I. M., Lange, M., Lique, C., MacGilchrist, G. A., Marsh, R., Mayorga Adame, C. G., McAdam, R., Nencioli, F., Paris, C. B., Piggott, M. D., Polton, J. A., Rühs, S., Shah, S. H., Thomas, M. D., Wang, J., Wolfram, P. J., Zanna, L., and Zika, J. D.: Lagrangian ocean analysis: Fundamentals and practices, Ocean Modelling, 121, 49–75, https://doi.org/10.1016/j.ocemod.2017.11.008, 2018.

Vastano, A. C. and Barron, C. N.: Comparison of satellite and drifter surface flow estimates in the northwestern Gulf of Mexico, Cont. Shelf Res., 14, https://doi.org/10.1016/0278-4343(94)90108-2, 1994.

Villas Bôas, A. B., Ardhuin, F., Ayet, A., Bourassa, M. A., Brandt, P., Chapron, B., Cornuelle, B. D., Farrar, J. T., Fewings, M. R., Fox-Kemper, B., Gille, S. T., Gommenginger, C., Heimbach, P., Hell, M. C., Li, Q., Mazloff, M. R., Merrifield, S. T., Mouche, A., Rio, M. H., Rodriguez, E., Shutler, J. D., Subramanian, A. C., Terrill, E. J., Tsamados, M., Ubelmann, C., and van Sebille, E.: Integrated Observations of Global Surface Winds, Currents, and Waves: Requirements and Challenges for the Next Decade, Frontiers in Marine Science, 6, https://doi.org/10.3389/fmars.2019.00425, 2019.